Torque Vectoring In Electric Vehicles

ISAH HASSAN

26006465 | Mechanical Engineering | Sheffield Hallam University

Dissertation submitted in partial fulfilment of the requirements of the degree of Bachelor of Engineering

Preface

This report describes project work carried out within the Department of Engineering & Mathematics at Sheffield Hallam University between October 2018 and April 2019.

The submission of the report is in accordance with the requirements for the award of the degree of Bachelor of engineering in Mechanical Engineering under the auspices of the University.

Acknowledgments

لَا إِلٰهَ إِلَّا ٱللهُ مُحَمَّدٌ رَسُولُ ٱللهِ

There is no God but Allah, Muhammad is the messenger of Allah

Alhamdulillah, First and foremost I would like praise Allah and thank him for his blessing, without his guidance none of this would be possible. I would like to also thank Mama for her endless love and support for without her I would be lost. I am indebted to Baba for pushing me to be the best person I can be and helping me achieve everything that I have. I am grateful for the endless support and encouragement from all of my family. Thank you to my best friend Ayesha for supporting me throughout my three years of university, being there for me no matter the situation and bringing me closer to Allah, I can't even begin to explain how much your actions mean to me. Thank you to Emily for the endless laughter you bring me, continuing support you give me and for being such an amazing best friend, I don't know what I'd do without you. I would also like to show gratitude and appreciation to the rest of my friends who have given me endless support and encouragement. Finally, I am greatly appreciative of my supervisor, Dr Basilio Lenzo. I appreciate your flexibility and willingness to help with any matter in this project. Thank you for the vast amount of knowledge, assistance and guidance provided when carrying out this dissertation played a large role in the completion of the project.

Abstract

In this report, a mathematical model of a vehicle is derived and designed using MATLAB and Simulink software to which a torque vectoring strategy is introduced to control the propulsion of the vehicles individual electric motors at each wheel. The development of this torque vectoring controller aimed to increase stability and dynamic performance of an electric vehicle. The report consists of a thorough literature review, studying mathematical modelling and a variety of yaw moment controls, followed by in depth testing of the designed PID controller using different manoeuvres to test its performance and finally concluding the efficiency of the controller and a discussion on how well it impacts the vehicles stability and dynamic performance.

Summary

The outline of this report includes the design of a torque vectoring controller, using the understeering gradient (k_u) to calculate a reference yaw rate, is implemented upon a designed double track model to attempt to control the yaw rate and therefore increase the stability and control of the vehicle. The project is separated into five key sections which all play a vital role in its completion:

- **Research -** The first section is comprised of an introduction into torque vectoring and its uses in today's age. This fragment covers the several types of TV systems along with their uses.
- **Mathematical Modelling -** The second section includes an introduction into mathematical modelling along with a derived and designed mathematical vehicle model, necessary for the implementation of a torque vectoring controller, and the functionally tests for this model.
- **Controller Design** – Thirdly, research into yaw moment control and its applications is completed. Using this research, a control strategy to function with the vehicle model is designed using the understeering gradient (k_u).
- **Testing & Comparison** – The testing of the functionality of this torque vectoring controller was carried out using four manoeuvres (step response, ramp response, single lane change and double lane change) followed by a functionality comparison against the previously designed controllers using different control strategies.
- **Conclusion** – The final section of this report concludes the whole design and implementation of the vehicle model and yaw rate controller along with a critique of the design and the overview of possible future work.

Contents

1. Introduction

Internal combustion engines (ICEs) are the main power source of today's vehicles. The drivetrain of ICE vehicles transfers engine torque to the rear, front or all wheels. In order to power ICE vehicles, it is necessary to use products extracted by fossil fuels, which tends to result in perpetuating the issues which are damaging to planet Earth such as excess production of air pollution, resulting in a global environmental problem. The electrification of vehicles produces a potential solution to aim to tackle these recent concerns of environmental pollution. With advanced evolution in today's battery technology, progressions in propulsion motors and larger integration with urban infrastructure, electric battery powered vehicles are growing resulting in a greener source of transport. (Chan, 2002) These advancements in electric technology allow for an electric vehicle with individually controlled powertrains, offering a new possibility in the improvement in dynamic behaviour due to higher controllability. Modern day technology presents many different control strategies in a vehicle aiming towards improving the lateral acceleration, stability and ride quality at high speeds, however, for electric vehicles integrated with individual electric motors, torque vectoring can be used. (Kaiser, 2015)

Torque vectoring (TV) describes the capabilities of controlling the torque transmission to individual wheels to influence the dynamics of the vehicle. Typically, the control strategy aims to apply different torques to each wheel to generate a change in the longitudinal forces applied on the tyres and producing a yaw moment. Direct yaw moment control (DYC) follows this same principle in using the longitudinal forces to control the yaw rate, whether it be through acceleration or deceleration (Fu, 2014). DYC consists of three stages; yaw rate measurement, comparison to a predefined optimisation reference and finally the control action on the vehicle. (Vianna, 2018)

1.1 Objectives

The scope of this project is to implement this modern concept of torque vectoring into a MATLAB and Simulink model of an electric vehicle in order to enhance the driving stability and safety without compromising the users driving experience. This model will be tested through a series of simple simulated manoeuvres measuring the effectiveness of the torque vectoring controller and how it has a greater efficiency and effectiveness compared to the control parameters of a conventional vehicle. The final stage of the project will be to critically compare the performance of the designed TV controller against other predesigned modelled. The followed workflow for developing this controller is shown in figure 1.1.

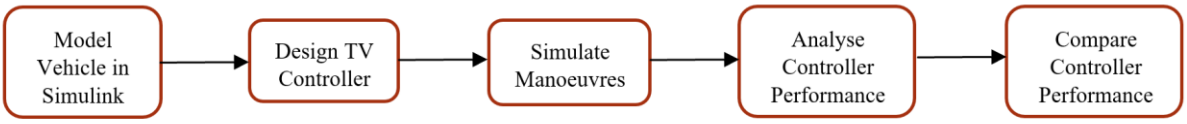

Figure 1.1: Project Workflow

2. Torque Vectoring

Torque vectoring is a system that aims to provide optimal dynamic performance for a vehicle at any given situation. It is a very important stability control method in current development. The fundamental aspect of torque vectoring is the generation of a difference of force between the right and left wheel, improving the performance when cornering (Gan, 2013). The vehicle torque distribution is performed using its breaks and propulsion system. A torque vectoring system works by controlling the magnitude and direction of the torque transmission between the right and left wheels. The driving force acts upon one wheel whereas the breaking force acts upon the other generating a difference in the driving force and generating a yaw moment which acts on the wheel. Therefore, when the TV transmission is zero, the engine torque is equally distributed between the two wheels. A TV system is capable of influencing the system in two ways. The first is the optimal distribution of the cornering forces amongst the front and rear wheels, the second is the optimum distribution of driving forces to which they expand to the cornering limit. (Stoop, 2014)

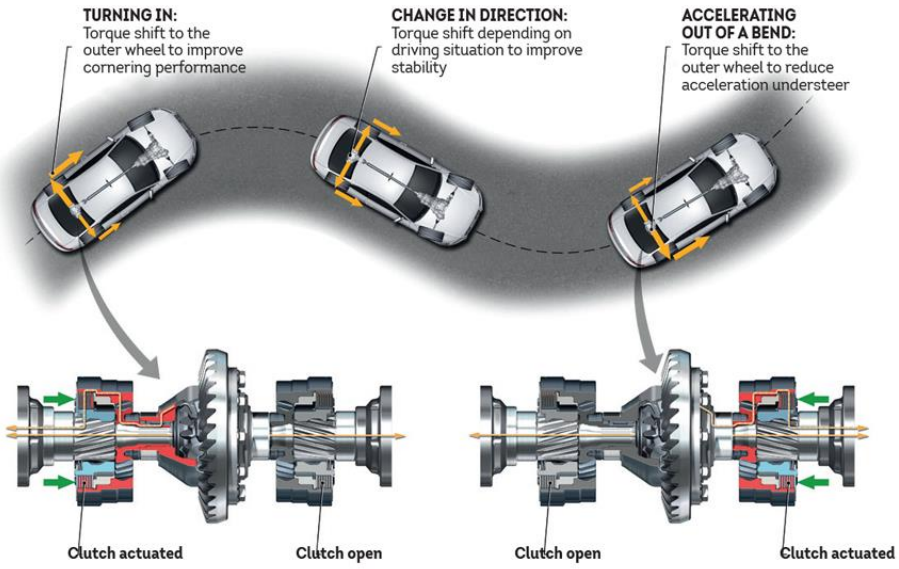

Figure 2.1: TV System (What is Torque Vectoring?, n.d.)

The topic of torque vectoring can be divided into three subsections: passive, active and electric.

2.1 Passive TV Systems

Often described as ‘differential breaking’ due to the generation of a breaking difference, passive torque vectoring systems introduces the yaw moment of a vehicle trough individual break torque distribution. Passive TV systems electronically sense the yaw rate and steering angle, consequently, using this information to control the individual wheels break pressure. The simplicity to this type of torque vectoring system largely relies on its simple installation as the only alteration is the control software if the vehicle is equipped with electric stability control and ergo, there isn’t a need for additional parts, resulting in no increase of cost. However, passive torque vectoring systems cannot generate yaw moment effectively during deceleration, resulting in a reduction of break abrasion and vehicle velocity. (Kaiser, 2015)

2.2 Active TV Systems

Active torque vectoring systems focus on distributing the engines torque to the wheels of the vehicle. Active differentials introduce additional gears and clutches distributing to the drive torque in the left and right wheels influencing the performance and movement of the vehicle. This type of torque vectoring system can be used in front or rear wheel drive systems, with a single active differential, along with four-wheel systems, which need the implementation of three active differentials, creating a higher intensity when influencing vehicle behaviour. Active torque vectoring systems have several advantages, the effectiveness and agility of the system is improved, the steering effort is reduced and there is no velocity loss. Disadvantages to this system include the purchase and introduction of additional parts for the active differential therefore increasing the cost and weight of the vehicle. (Belisso, 2009)

2.3 Electric TV Systems

The final type of torque vectoring system requires a 2nd generation vehicle. 2nd generation vehicles are electric vehicles equipped with two or four electric motors controlling the wheels independently allowing the generation of positive and negative torque. Electric torque vectoring systems are a combination of passive and active torque vectoring systems; hence, the generation of high yaw moments can be achieved through fast and accurate control of the electric motors increasing the efficiency of the vehicle. Individual wheel propulsion devices allow effective stability control in electric vehicles through selective torque distribution, unlike the typical friction-based control in conventional vehicles which relies on a standard internal combustion engine, with integrated active differentials and hydraulic breaks. Torque vectoring offers a capability for each wheel of a vehicle to each have an individual torque distribution which in turn has a direct impact on the yaw moment, the fundamental awareness behind many existing vehicle control systems. Yaw moment generation is achieved in these vehicles through an increase in the overall breaking torque of the vehicle, therefore leading to a decrease of speed. Torque vectoring aims to apply this yaw moment generation in a way where the reduction of speed does not need to be as significant without compromising the vehicles safety and handling. Controlling the yaw moment through and electric motor allows the incorporation of greater functionalities of the vehicle such as the comfort, safety and fun to drive enhancements (MicheleVignati, 2016). The main advantage of using individual motors at each wheel is the ability to apply a positive torque to one side whilst applying a negative torque to the other, therefore offering a larger torque vectoring potential and adding a degree of freedom to the system. However, these systems do have their drawbacks. The main disadvantage is the cost of the components in an electric torque vectoring system, there is also that of the complexity of the system hence the difficulty to run the system and finally the performance limitations of the torque vectoring system. (Kaiser, 2015)

2.4 In wheel motors (IWMs)

IWMs are electric motors positioned individually inside of each wheel of a vehicle. Introducing individual motors, the wheel torques can be independently controlled, allowing the better use of dynamic control systems. However, there are still disadvantages involved such as the increase in unsprung mass.

2.4.1 Installation

There are two methods in which IWMs can be linked to the wheels of a vehicle, illustrated in figure 2.2. The first is indirect drive in wheel motors with a gear reduction, with fixed gearing and the second is direct drive in wheel motors without any gear reduction. The indirect drive

configuration is used with a high-speed permanent magnet inner rotor type. In the right-hand side configuration, the speed of the wheel is equal to the speed of the motor, resulting in a bigger and heavier motor. Yet, the use of no transmission gears results in a reduction of complexity and the avoidance of transmission losses. (Vos, 2010)

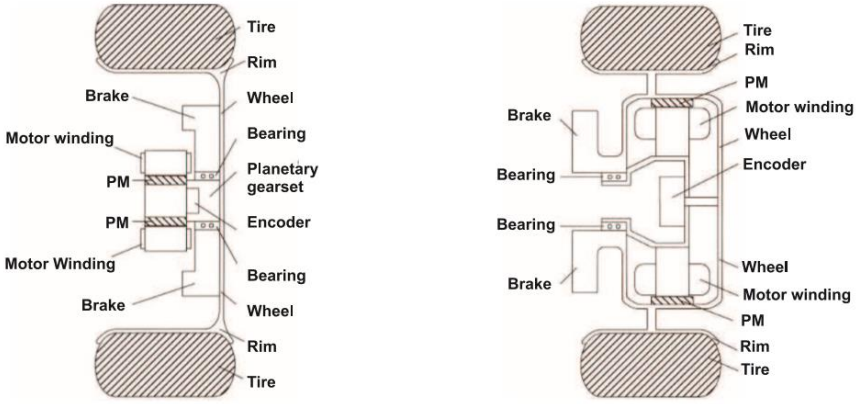

Figure 2.2: Indirect (left) and Direct (right) in wheel motor configurations

2.4.2 Advantages and disadvantages

As mentioned previously, the use of individual electric motors provide the possibility of independent control of the torque allocation to each wheel. The system also eliminates the necessity of differentials and drive shafts, ergo, reducing the size and weight along with the transmission losses. Additionally, using IWMs gives more room in the interior of a vehicle. (Vianna, 2018)

Nevertheless, a large disadvantage of using IWMs is the increased unsprung mass, degrading the ride comfort and road holding. Due to this factor there is also sacrifices in the following aspects:

- Transmissibility ratio – The response from the sprung mass from an excitation produced from the road.
- Dynamic tyre deflection ratio – The displacement of unsprung mass over a road input, measuring the wheel load dynamics and therefore the capability of road holding.
- Travel suspension ratio – The ratio of maximum displacement between sprung mass and unsprung mass over a road excitation.
  (Anderson, 2011)

2.5 Types of Steering

Improving the safety and performance of a vehicle includes counteracting the problems that cornering can present; understeer and oversteer, these issues are highlighted below.

2.5.1 Understeer

Understeer occours when the front two tyres lose grip on the road surface causing the vehicle to push towards the outside of the curb rather than follow the corners curvature. The cause of understeer is generally from when the front wheels are directed to turn whilst the car is undergoing a large amount of acceleration or deceleration.

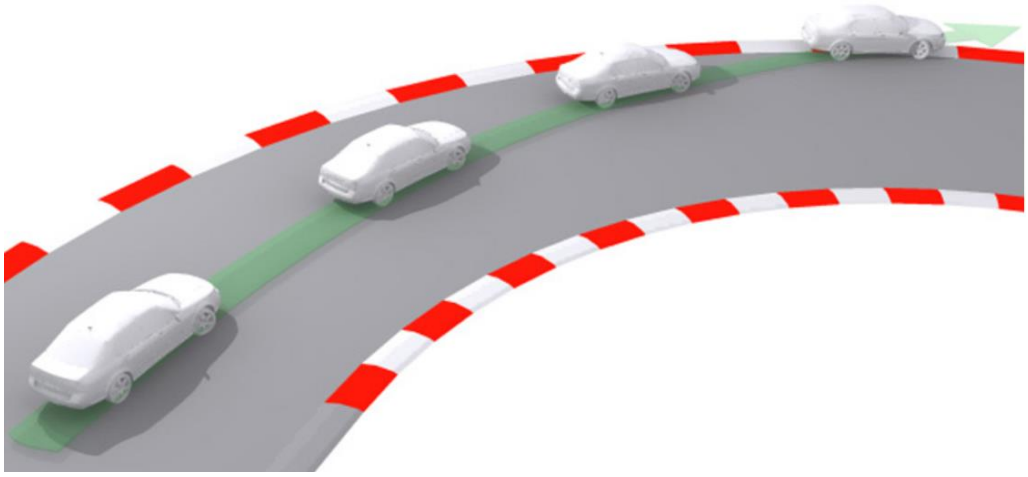

Figure 2.3: Understeering (Collins, 2019)

2.5.2 Oversteer

This principle follows similar circumstances to that of understeer but instead effecting the rear end of the vehicle. Oversteer is the tendency for the back end of the vehicle wanting to overtake the front whilst cornering. This happens when the driver of the vehicle applies more pressure than the tyres can handle causing the car to slip and push in the opposite direction to the corner, kicking the rear end of the car out. (Collins, 2019)

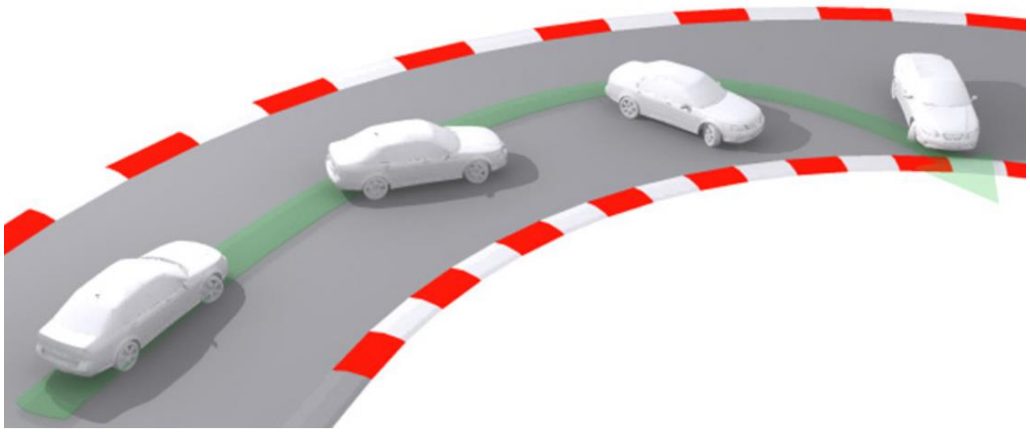

Figure 2.4: Oversteering (Collins, 2019)

3. Mathematical Modelling

A mathematical model describes the beliefs and functionalities of this world and converts them into mathematical language. Mathematical modelling presents many advantages when simulating real life scenarios. It has well distinct rules for manipulation making it a very concise and precise language, helping the formulation of ideas and the identification of underlying assumptions. Another advantage of using this simulation method is the ease of use due to no physical experiments being needed. This removes risks from real life experiments as well as reducing the cost of producing a system.

3.1Vehicle Dynamics

3.1.1 Vehicle Scheme

Mathematical modelling of a vehicle is a significant factor in the optimisation of the dynamics of an electric vehicle, yet it should not be too complex. There are many ways in which a vehicle model can be created, however all models should be designed so that they can reliably predict the behaviour of a real vehicle. There are two main assumptions when considering the mathematical design of a vehicle. These assumptions are regarding the operating conditions and physical modelling.

Operating conditions can be divided in to three main sections:

- Performance – The vehicle is moving linearly along a flat road surface, possibly breaking or accelerating.
- Handling – the turning of the vehicle is always on a flat road and is generally with a nearly constant forward velocity.
- Ride – the vehicle is progressing along a straight bumpy road with a constant linear velocity.

In real situations and conditions, the operation conditions are a variation and mixture of all three sections.

The physical modelling of the vehicle may coincide with the following features:

- The body is to be modelled as a single rigid body.
- Only one degree of freedom should be allowed when the wheels are linked to the body.
- The steering wheels angular position (δ_v)should be the main determinant of the steering angle of both front wheels.
- The mass of the wheels (unsprung mass) should be significantly small when compared to the vehicle body (sprung mass).
- The tyres of the vehicle should contain air or gas under pressure (pneumatic tyres).
- The suspension system of the vehicle should contain springs and dampers and the two suspension systems should be connected by the same axle.
- There may be a possibility of added aerodynamic features that may significantly affect the downward force.

It is also essential for a mathematical vehicle model to follow some fundamental geometrical parameters shown in figure 3.1:

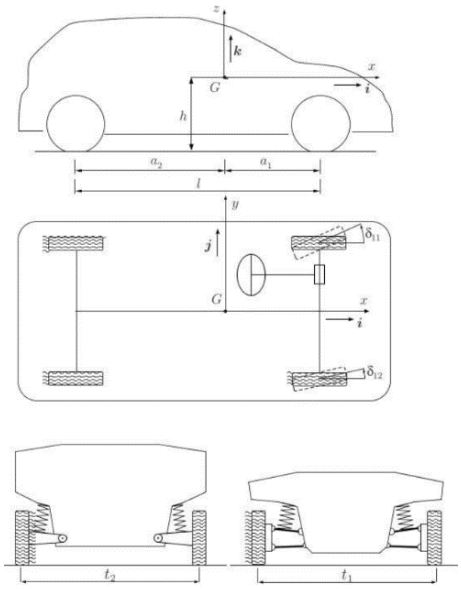

Figure3.1: Vehicle Schematic (Guiggiani, 2014)

- The vehicle has a longitudinal axis, x, and therefore should be heading in the i direction.
- The centre of gravity G of the whole vehicle is at height h from the road plane.
- a_1 and a_2 correspond to the longitudinal distances of G from the front and rear axles.
- Therefore the wheel base $l = a_1 + a_2$
- t_1 and $t_1$are the front and rear tracks.
- The linkage geometry of the front and rear suspension.
- The position of the steering wheel in relation to each wheel.
- A swing arm rear suspension with double wishbone front suspension.

3.1.2 Handling and Performance

Handling and performance are the essential factors in the creation of a vehicle model. In order to understand and develop these the dynamics the system must be studied. When studying these factors, the paving of the road is assumed to be perfectly flat with no uniform features. Using these assumptions, the vehicle model should fulfil the assumptions made in the physical modelling with the addition of:

- The suspension deflection of the vehicle being negligible.
- The vertical deformations of the tyres are insignificant.
- A small steering angle.
- The steering system is perfectly rigid.
    - The system is assumed rigid to simplify the dynamics of the vehicle, removing aspects such as caster angle and kingpin inclination.

The extra assumption added amount, mathematically, to allowing the vehicle to always be in its reference configuration, keeping a_1, a_2, l, t_1, t_2 constant in vehicle motion, with the exclusion of δ_{11} and δ_{12} (steering angles).

The net effect of these influences is that the body of the mathematically modelled vehicle has a planar motion parallel to the road. (Guiggiani, 2014)

4. Single Track Model

Single track models are the most commonly used vehicle model when inspecting the lateral velocity of a body. The basic principle of this model is merging the wheels of a single axle, displayed in figure 4.1. The model compromises the dynamics by assuming the wheels on the left and right produce the same lateral forces. This lateral force is therefore assumed linear to the tyre slip angles of the vehicles.

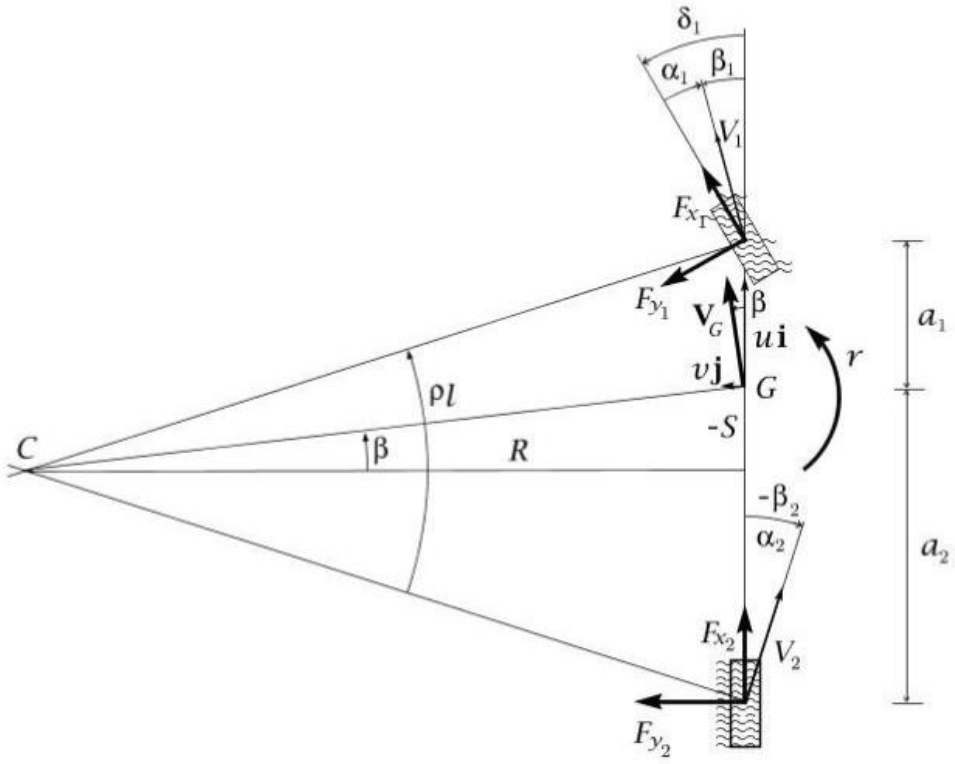

Figure 4.1: Single Track Model (Guiggiani, 2014)

The single-track model was initially designed on Simulink as a basis for the double track model modelled in the following section. The governing equations for this mathematical model were found using the book 'The science of vehicle dynamics' and are derived using three fairly simple equations.

- The two equilibrium equations:

$$m(\dot{v} + ur) = Y = Y_1 + Y_2 = ma_y \tag{4.1}$$

$$J_z\dot{r} = N = Y_1a_1 - Y_2a_2 \tag{4.2}$$

- Two congruence equations:

$$\alpha_1 = \delta_v\tau_1 - \frac{v + ra_1}{u} \tag{4.3}$$

$$\alpha_2 = \delta_v\tau_2 - \frac{v - ra_2}{u} \tag{4.4}$$

- Two constitutive equations (axle characteristics):

$$Y_1 = Y_1(\alpha_1) \tag{4.5}$$

$$Y_2 = Y_2(\alpha_2) \tag{4.6}$$

Two derived equilibrium equations are both first order differential equations. Therefore, the model is a dynamic system comprised of two state variables $v(t)$ and $r(t)$. The two congruence equations and two constitutive equations must be placed into the two equilibrium equations to find the dynamic governing equations of a single-track model. (Guiggiani, 2014)

$$\dot{v} = \frac{1}{m}\left[Y_1\left(\delta_1\tau_1 - \frac{v + r_{a_1}}{u}\right) - Y_2\left(\delta_v\tau_2 - \frac{v - ra_2}{u}\right)\right] - ur \tag{4.7}$$

$$\dot{r} = \frac{1}{J_z}\left[a_1 Y_1\left(\delta_1\tau_1 - \frac{v + r_{a_1}}{u}\right) - a_2 Y_2\left(\delta_v\tau_2 - \frac{v - ra_2}{u}\right)\right] \tag{4.8}$$

5. Double Track Model

The mathematical modelling of the vehicle would be essential in the design of the torque vectoring controller. A double track model presents a dynamic system providing two state variables, $v(t)$ and $r(t)$.

The double track model presents a two-dimensional rigid body which moves in the x and y plane. This model covers the lateral, longitudinal and yaw movement around the centre of gravity, neglecting the vertical direction transversal movements along with rotational movements around the x and y axis. In a DTM, static and normal forces cover the wheel dynamics in the lateral and longitudinal directions.

The vehicles dynamics equations were derived from the diagram shown in figure 5.1. The diagram provides a schematic of the main components acting upon a double track vehicle. The initial equations were comprised from equating the forces on the vehicle along with the moments and applying them into separate equations.

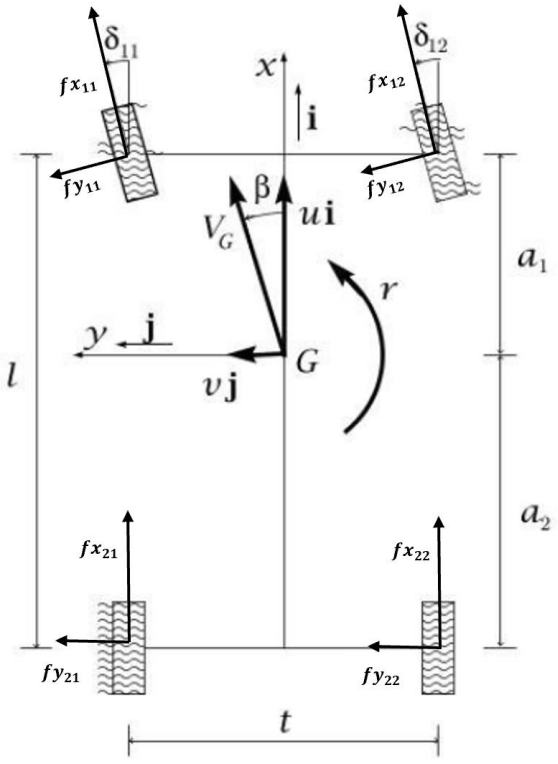

Figure 5.1: Double Track Model (Guiggiani, 2014)

5.1 Longitudinal Dynamics

The development of a double track model involves viewing the vehicles movement laterally and highlighting the forces which are acting upon it. The main contributing forces acting on a vehicle are the aerodynamic drag force (F_d) and the longitudinal forces for both front and rear wheels. These factors make up the equilibrium equation for the longitudinal velocity:

$$ma_x = X_1 + X_2 - F_d \qquad (5.1.1)$$

The drag is an aerodynamic resistance force that opposes a rigid body as it passes through the air. Introducing drag into the double track model will increase the reliability of the model included in the introduction of a drag force. The equation of the drag force is:

$$F_d = \rho A C_x u^2 \tag{5.1.2}$$

Exploiting each tyres contribution to the vehicles dynamics by resolving the forces acting upon them, equation 5.1.3 can be derived for the lateral dynamic equilibrium equation:

$$v = \frac{\dot{u}}{r} - \frac{r(F_{x_{11}}\cos(\delta_v) + F_{x_{12}}\cos(\delta_v) + F_{x_{21}} + F_{x_{22}} - F_{y_{11}}\sin(\delta_v) - F_{y_{12}}\sin(\delta_v))}{m} \tag{5.1.3}$$

These equations together provide a good mathematical model of a vehicle, however, the forces in the x and y direction would need to be defined accurately for the system to be operable.

5.2 Lateral Dynamics

The yaw of a vehicle, as discussed later in this report, provides fundamental indication of the vehicle's conditions. The schematic diagram (figure 5.1) presents the yaw moment at the mass centre of the vehicle (G), considering all longitudinal and lateral forces. Equation 5.2.1 is derived using the lateral dynamic analysis, expressing displacement of the centre of gravity along the vehicles y axis. The resulting equilibrium equation defining the lateral dynamics is:

$$ma_y = Y_1 + Y_2 \tag{5.2.1}$$

Resolving all forces acting on the vehicle schematic results in equation 5.2.1 becoming equation 5.2.2:

$$u = \frac{r(F_{x_{11}}\cos(\delta_v) + F_{x_{11}}\cos(\delta_v) + F_{y_{11}}\cos(\delta_v) + F_{y_{12}}\cos(\delta_v) + F_{y_{21}} + F_{y_{22}})}{m} - \frac{\dot{v}}{r} \tag{5.2.2}$$

The equilibrium equation defining the moments acting upon the system is provided in 5.2.3:

$$J_z\dot{r} = Y_1 a_1 + Y_2 a_2 + \Delta X_1 t_1 + X_2 t_2 \tag{5.2.3}$$

Again, exploiting and resolving each tyre force, the equation deriving the yaw moment can be defined.

$$\frac{\begin{array}{c}\frac{t}{2}\left(F_{x_{11}}\cos(\delta_v) - F_{x_{11}}\cos(\delta_v) + F_{x_{21}} - F_{x_{22}} + F_{y_{11}}\sin(\delta_v) - F_{y_{12}}\sin(\delta_v)\right) \\ +a_1\left(F_{x_{11}}sin(\delta_v) + F_{x_{12}}sin(\delta_v) + F_{y_{11}}cos(\delta_v) + F_{y_{12}}cos(\delta_v)\right) \\ +a_2\left(-F_{y_{21}} - F_{y_{22}}\right)\end{array}}{J_z} = \dot{r} \tag{5.2.4}$$

All tangential grip forces presented in each lateral and longitudinal dynamic equation are defined by:

$$X_1 = X_{11} + X_{12} \tag{5.2.5}$$

$$X_2 = X_{21} + X_{22} \tag{5.2.6}$$

$$Y_1 = Y_{11} + Y_{12} \tag{5.2.7}$$

$$Y_2 = Y_{12} + Y_{22} \tag{5.2.8}$$

5.3 Lateral Forces

In order to introduce the lateral forces of the vehicle model, the tyre kinematics must be brought into the system, therefore, resulting in the forces $F_{y_{11}}$, $F_{y_{12}}$, $F_{y_{21}}$ and $F_{y_{22}}$ being derived.

5.3.1 Tyre Kinematics

The wheels kinematics play a large role in the vehicles dynamics as they have a strong effect on the exerted forces from the tyres, hence why engineers need to consider these factors.

The centre velocity of the front left wheel is calculated using the following equation:

$$V_{11} = V_G + r\boldsymbol{k} \times GP_{11} = (u\boldsymbol{i} + v\boldsymbol{j}) + rk \times (a_1\boldsymbol{i} + \frac{t_1}{2}\boldsymbol{j}) \tag{5.3.1}$$

Implementing this calculation onto all wheel centres results in equations 5.3.2 to 5.3.5.

$$V_{11} = \left(u - \frac{rt_1}{2}\right)\boldsymbol{i} + (v + ra_1)\boldsymbol{j} \tag{5.3.2}$$

$$V_{12} = \left(u + \frac{rt_1}{2}\right)\boldsymbol{i} + (v + ra_1)\boldsymbol{j} \tag{5.3.3}$$

$$V_{21} = \left(u - \frac{rt_1}{2}\right)\boldsymbol{i} + (v - ra_1)\boldsymbol{j} \tag{5.3.4}$$

$$V_{22} = \left(u - \frac{rt_1}{2}\right)\boldsymbol{i} + (v - ra_1)\boldsymbol{j} \tag{5.3.5}$$

Ergo, the angles needed between the vehicle's longitudinal axis $\boldsymbol{i}$ and $\boldsymbol{V_{ij}}$ can be calculated through equations 5.3.6 to 5.3.9:

$$\tan(\hat{\beta}_{11}) = \frac{v + ra_1}{u - \frac{rt_1}{2}} = \beta_{11} = \tan(\delta_{11} - \alpha_{11}) \tag{5.3.6}$$

$$\tan(\hat{\beta}_{12}) = \frac{v + ra_1}{u - \frac{rt_1}{2}} = \beta_{12} = \tan(\delta_{12} - \alpha_{12}) \tag{5.3.7}$$

$$\tan(\hat{\beta}_{21}) = \frac{v + ra_2}{u - \frac{rt_2}{2}} = \beta_{21} = \tan(\delta_{21} - \alpha_{21}) \tag{5.3.8}$$

$$\tan(\hat{\beta}_{22}) = \frac{v + ra_2}{u - \frac{rt_2}{2}} = \beta_{22} = \tan(\delta_{22} - \alpha_{22}) \tag{5.3.9}$$

The forces acting in the y direction can be defined through a simple equation, through the integration of the slip and steering angles of each individual wheel.

$$\alpha_{ij} = \delta_{ij} - \beta_{ij} \tag{5.3.10}$$

Hence, using the same steering angle for the front two wheels and a steering angle of 0 for the back two, the final equations for the y directional forces were derived.

$$F_{y_{11}} = c_1\left(\delta_v - \frac{v + ra_1}{u - r\frac{t}{2}}\right) \tag{5.3.11}$$

$$F_{y_{12}} = c_1\left(\delta_v - \frac{v + ra_1}{u + r\frac{t}{2}}\right) \tag{5.3.12}$$

$$F_{y_{21}} = 0 - c_2\left(-\frac{v - ra_1}{u - r\frac{t}{2}}\right) \tag{5.3.13}$$

$$F_{y_{22}} = 0 - c_2\left(-\frac{v - ra_1}{u + r\frac{t}{2}}\right) \tag{5.3.14}$$

5.4 Longitudinal Forces

The forces in the x direction can all be derived using the same values. When simulating the vehicle system, a constant velocity of $25m/s$ would need to be achieved therefore the forces in the x direction would need to provide adequate force to achieve this velocity. In order to achieve this force, the lateral velocity would need to be taken and subtracted from a reference velocity of $25m/s$, therefore giving an error value. The output error was sent through a PID controller to provide a directional x force which will maintain this velocity.

$$e = u_{ref} - u_{actual} \tag{5.4.1}$$

The PID (Proportional, Integral and Derivative) controller is a form of feedback control that aims to reduce the error in a system. Entering specific values for the proportional and integral values provides a control system for the longitudinal velocity. In terms of the Double Track Model the PID controller will reduce the error signal in the lateral velocity therefore allowing the system to run at a constant of $25m/s$. (Sena TEMEL, 2015)

5.4.1 Drag Force

Subtracting the resulting drag force value, explained in section 5.1, from the output of the PID controller simulated the mathematical equivalent of the force drag resistance force.

5.5 Acceleration & Radii of Curvature

The angular acceleration of the vehicle is simply given by the following equation:

$$\Omega = \dot{r}\dot{k} = \dot{\psi}k \tag{5.5.1}$$

The absolute acceleration (a_G) of G presents a more involved evaluation of acceleration:

$$a_G = \frac{dV_G}{dt} = \dot{u}\boldsymbol{i} + ur\boldsymbol{j} + \dot{v}\boldsymbol{i} - vr\boldsymbol{j} = (\dot{u} - vr)\boldsymbol{i} + (\dot{v} - ur)\boldsymbol{i} = a_x\boldsymbol{i} + a_y\boldsymbol{j} \tag{5.5.2}$$

Through equation 5.5.2 the longitudinal and lateral velocity of the vehicle can be defined.

Measuring the functionality of the model can be completed through the monitoring of the longitudinal acceleration (a_x) and the lateral acceleration (a_y). The two governing equations for these accelerations are:

$$a_x = \dot{u} - vr \tag{5.5.3}$$

$$a_y = \dot{v} + ur \tag{5.5.4}$$

5.6 Steering Ratio

The steering wheel is the physical part of the system which is manipulated in order to turn the vehicle. Most modern vehicles require several rotations of the steering wheel in order to reach the maximum wheel angle. The steering ratio is the number of steering wheel rotations that is necessary to elicit a certain movement in the wheels. This value is typically measured in degrees but expressed as a ratio. The lower the steering ratio the more precise the turning will be. When designing a vehicle, the steering ratio is an aspect which needs a lot of consideration as it influences the vehicles handling and performance. This ratio along with the ease of steering is dependent upon a variety of factors which include; the steering wheel size, the gear size in the steering gear, the steering linkage angle, frontal weigh of the vehicle, size and shape of the steering arms and lastly whether the vehicle is front or rear wheel drive. The ratio inputted in to the double track model, just after the step block, was an average value, discovered through research, to be $1:15$. (PistonPuff, 2017)

5.7 Final Model

The final Simulink model is presented in figure 5.2. The details of this model are included in the appendix.

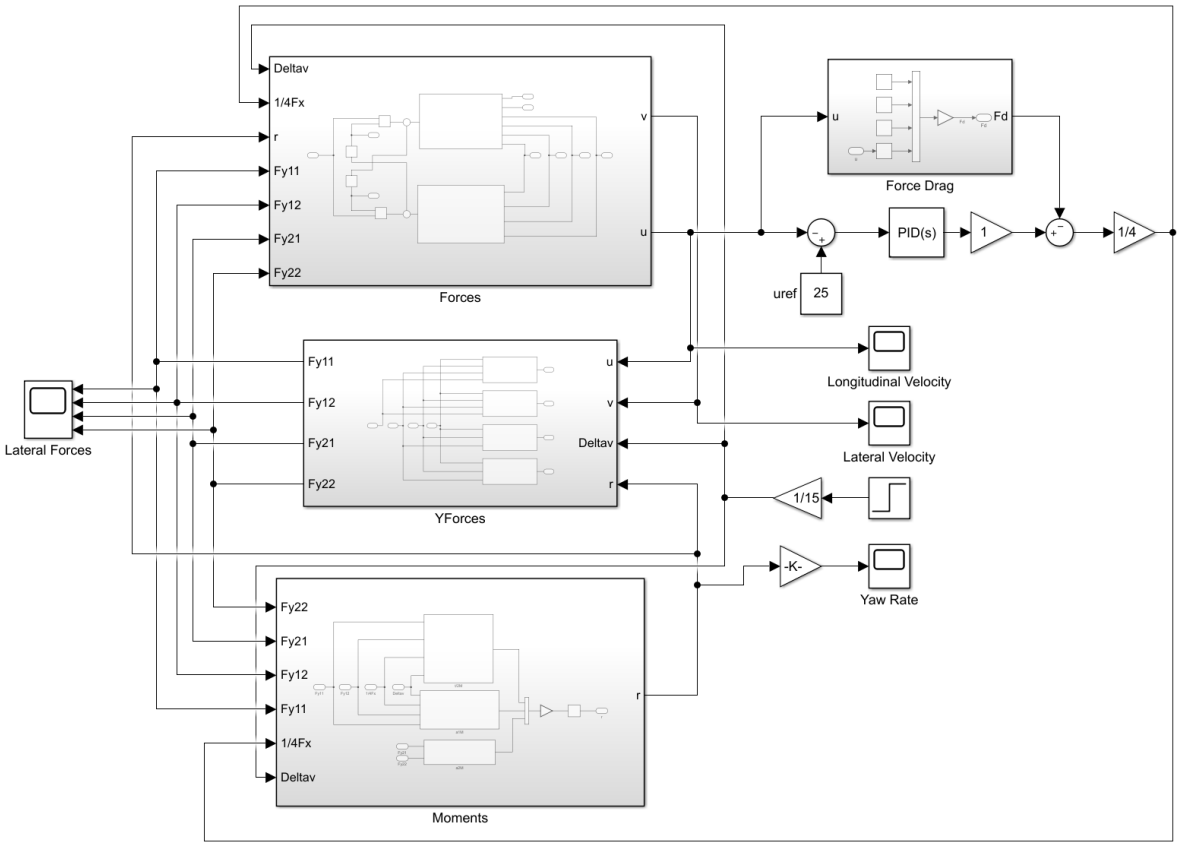

Figure 5.2: Double Track Model in Simulink

5.8 Parameters

The parameters using for the double track model were derived using a final masters torque vectoring thesis. (Ghezzi, 2017)

Table 5.1: Vehicle input parameters

Symbol	Value	Comment
a_1	$1.04m$	Longitudinal distance of the front axle from the centre of gravity.
a_2	$1.56m$	Longitudinal distance of the rear axle from the centre of gravity.
C_1	$70{,}000N$	Front axle cornering stiffness
C_2	$84{,}000N$	Rear axle cornering stiffness
t	$1.445m$	Front axle width
m	$1410kg$	Vehicle Mass
ρ	$1.225kg/m^3$	Density of air
A	2.2916	Frontal surface area
C_x	0.29	Coefficient of Drag

5.9 Mathematical Model Conclusion

The design of the double track model incorporated many of the necessary aspects of a real-life four-wheel drive vehicle. The mathematic equations which make up the system were given enough detail to label the model reliable when simulating different manoeuvres. However, in order to confirm this, the double track model will need to be tested to prove it is sufficient enough to have a yaw rate controller implemented into it.

6. Mathematical Model Results

The testing for the double track model, using the parameters stated in the previous section, would prove whether the system functioned properly according to vehicle dynamic laws. The system would need to function under several conditions. Hence when testing the necessary parameters, the model was simulated using steering angles of $\pm 50°, \pm 90°$ and $\pm 130°$.

6.1 Longitudinal Velocity

The desired longitudinal velocity for the double track model was $25m/s$. This was controlled using a simple PID controller, altering the integral and derivative gain. Figure 6.1 presents the graphs of lateral velocity when the model is simulated using the selected steering angles. The graphs represent conformation that the system able to control a longitudinal velocity, of $25m/s$, at any steering angle allowing the double track model to function correctly in terms of controlling the longitudinal velocity.

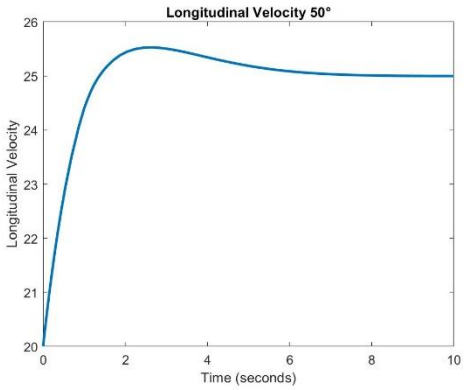

a) 50° Steering angle

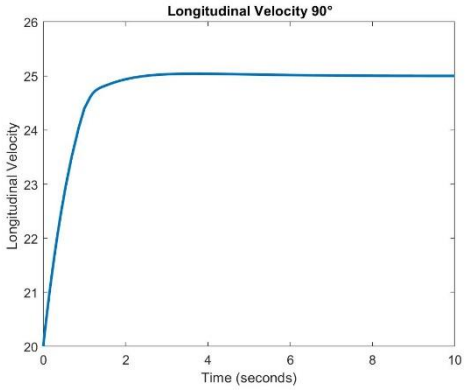

b) 90° Steering angle

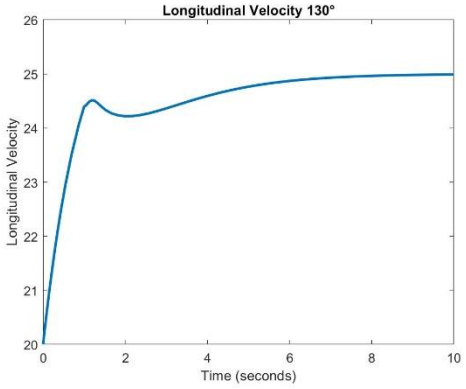

c) 130° Steering angle

Figure 6.1: Longitudinal Velocity Control

6.2 Yaw Rate

The yaw rate of the model is the main parameter of the double track model as it is the part of the system which associates it to the yaw control strategy presented at a later stage in this report. Presented below, are graphs showing the systems yaw rate behaviour at steering angles of $\pm 50°, \pm 90°$ and ± 130. The yaw rate of the system can be identified as functioning due to the yaw rate at each steering angle reaching a final value.

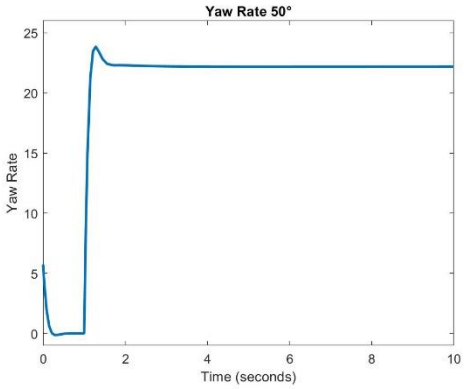

a) 50° Steering angle

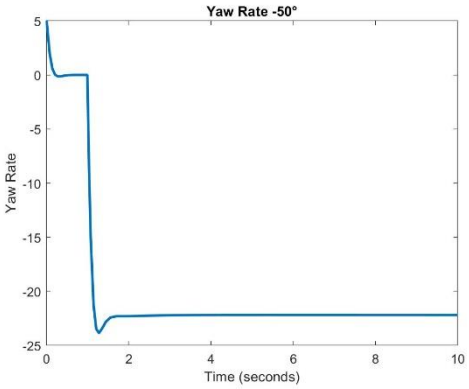

b) -50° Steering angle

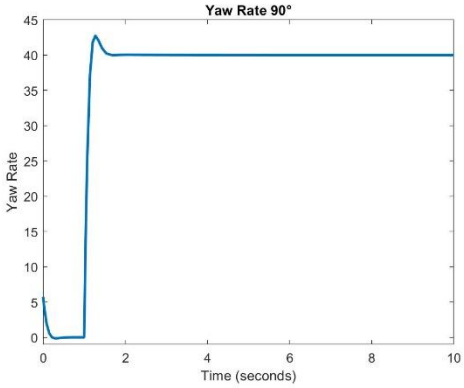

c) 90° Steering angle

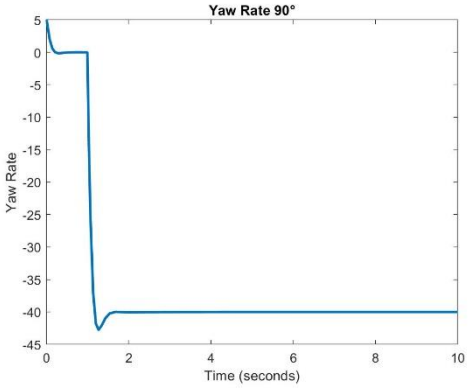

d) -90° Steering angle

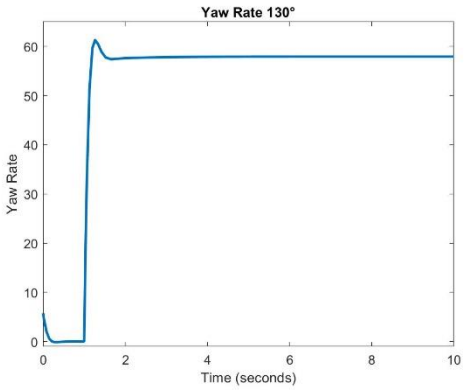

e) 130° Steering angle

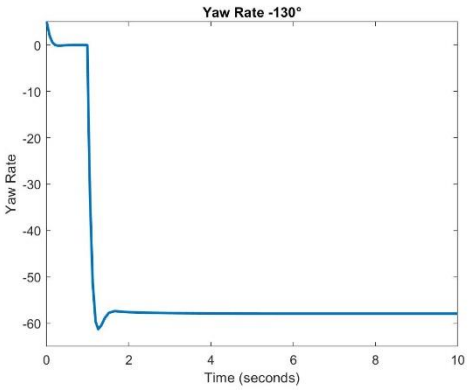

f) -130° Steering angle

Figure 6.2: Yaw Rate

6.3 Lateral velocity

The next important monitored value of the double track model is the lateral velocity. This parameter varies as the steering angle changes from 0° to 130°. Each lateral velocity simulation presents a final value connoting the system is functioning as expected.

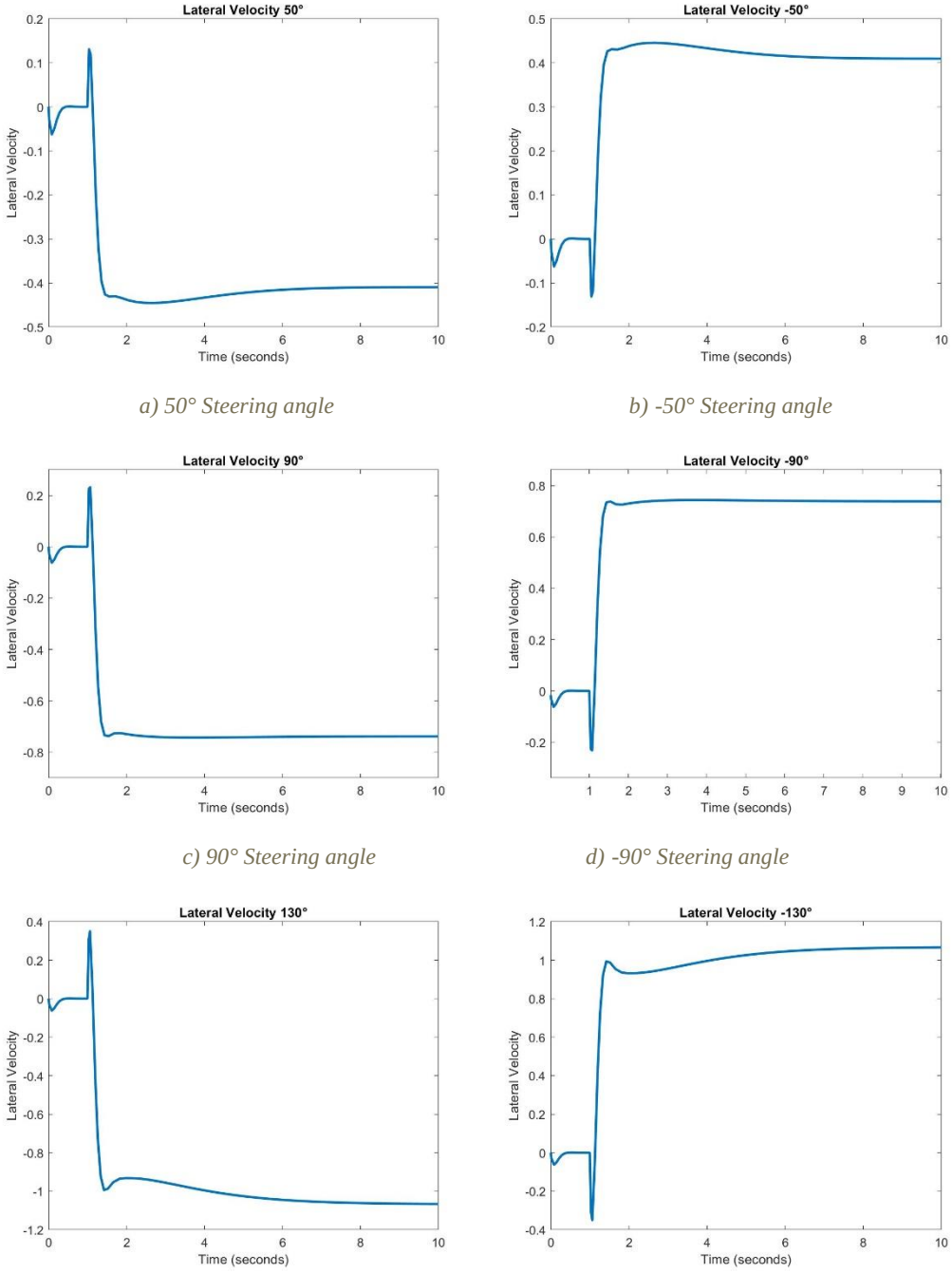

a) 50° Steering angle

b) -50° Steering angle

c) 90° Steering angle

d) -90° Steering angle

e) 130° Steering angle

f) -130° Steering angle

Figure 6.3: Lateral Velocity

6.4 Longitudinal Tyre Forces

The final monitorisation parameter of the vehicle model is the tyre forces. Presented in figure 6.4 is the amount of tyre force applied to each wheel. The longitudinal force distribution of each wheel was observed to be significantly more in the front two wheels than the rear two for all steering wheel angles. Monitoring these forces also showed each wheel reaching a steady state value proving the systems functionality and reliability.

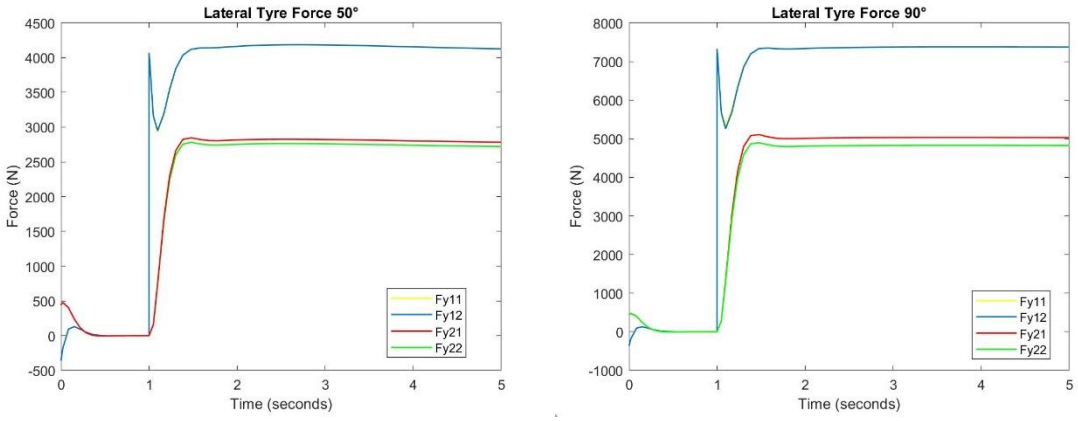

a) 50° Steering angle *b) 90° Steering angle*

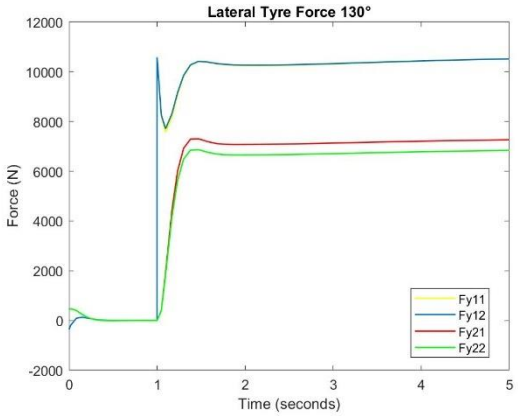

c) 130° Steering angle

Figure 6.4: Lateral Tyre Forces

6.5 Mathematical Model Results: Conclusion

All the observed parameters of the double track mathematical model follow the expected dynamics laws. Each parameter is capable of reaching a steady state value at a reasonable time under the different steering angles which were inputted into the system. Therefore, confirming the vehicle model is fully functional. Thus, torque vectoring algorithm can be designed to control these parameters and potentially improve the systems dynamic performance.

7. Yaw Moment Control

Yaw rotation simply indicates movement around the yaw axis of a rigid body that alters the direction it is moving, left or right. The yaw rate of a vehicle is the angular velocity of its rotation, commonly measured in radians per second. Many researchers have reported that the direct yaw moment is an effective method of controlling the movement of the vehicle about the yaw axis improving the vehicle's dynamic performance under a variation of road conditions. (Hall, 2015)

Controlling the direct yaw moment is a significant factor in the design of electric vehicles due to the installation of the extra components, such as the heavy battery boxes and electric motors, shifting the centre of gravity to an inconvenient position, causing the vehicle to oversteer. Therefore, additional stabilising mechanisms would need to be introduced to improve the dynamics performance of the vehicle.

The primary objective of controlling the direct yaw moment is to enhance the vehicles response by removing excess critical understeer. Hence, increasing the agility, improving the stability of the vehicle under critical conditions to avoid the vehicle spinning out, linearising the lateral acceleration of the vehicle and finally to minimise the vibrational behaviour with the longitudinal acceleration. (Vianna, 2018)

7.1 Previous Yaw Control Methods

Prior to direct yaw control systems being implemented into vehicles via individual electric motors, more simple approaches were developed to control these motors. These methods were the Ackermann method and the equal torque method.

7.1.1 Ackermann Method

Applying this method into vehicles requires a great deal of knowledge regarding the speed of the wheels and the steering wheel angle. This is due to the Ackerman method using analytical derivations calculating the rotational speed of the wheels using a kinematic condition. This essentially means the controller will calculate the reference of the inner and outer wheel velocities when cornering and act according to the results. The aim of the Ackerman method is to control the angular velocity of the wheels and not the yaw rate. The method has been known to work well especially at low speeds, due to its basis upon kinematic equations. When calculating at higher speeds, the method proves not to be as effective. (Fu, 2014)

7.1.2 The Equal Torque Method

The equal torque method aims to control each independent electric motor by giving the same amount of torque to the two electric machines. Essentially, the system functions similar to an open differential, allowing speed differentiation whilst keeping an equal torque at each wheel (no direct yaw moment control is present due to there being no active yaw moment generation). Using the ETM increases an electric vehicle cornering performance to that equivalent of an ICE vehicle supporting an open differential. This yaw control method is one of the simplest approaches in controlling individual electric motors, however, it doesn't exploit their full potential due to no direct yaw control. (Fu, 2014)

7.2 Yaw Control Methods

The previous yaw moment control methods mentioned have their limitations, hence why there is a desire to develop new control strategies that will explore the advantages of using independent motors. New methods consider the full vehicle dynamics and aim to control the

dynamics of the vehicle according to a reference point, working continuously, therefore generating the desired dynamics.

There are several control laws developed for torque vectoring. The most frequently used control strategies consist of the following methods.

7.2.1 Feed Forward Control

This strategy is based on operating the torque distribution in the right and left side of the vehicle using an open loop scheme. The yaw moment desired is described often as

$$M_z = g(v_x)\delta \tag{7.2.1}$$

Where M_z represents the desired yaw moment, δ represents the steering angle of the vehicle and g is a nonlinear function dependent on the longitudinal velocity v_x.

Using a feed forward control presents several advantages such as its low computational effort along with its simple implementation whilst providing a fast and accurate performance for the vehicle. However, the system does have drawbacks such as its sensitivity to noise and model variance. This system improves the overall performance of a closed loop system, but it is generally more beneficial to introduce feedback control for parameter variations. Combined solutions of the feed forward control and feedback control improve the performance of closed loop systems and deal with the system, parameters or disturbances. (Kaiser, 2015)

7.2.2 PID Control

A proportional integral and derivative (PID) controller is the most commonly used control parameter in practical applications. The control loop feedback mechanism works by calculating the difference between the process variable (actual yaw rate) and the desired setpoint (reference yaw rate). This value is taken as the error in which the controller tries to minimise this value through the adjustments of a manipulated variable. The algorithm which the PID controller is based upon three constant parameters, stated previously, proportional integral and derivative values. The interpretation of these values can be simply put in terms of time. The proportional gain depends upon the current error value, the integral gain relies on the accumulation of previous errors and finally, the derivative gain predicts the future errors. This type of controller is a straightforward but effective method in introducing yaw control whilst also having a simple application. (Kou, 2010)

7.2.3 Sliding Mode Control

Sliding mode control uses a nonlinear control method which alters the dynamics of the vehicle through the application of a control signal which is discontinuous. This signal forces the body to slide across a defined surface. SMC systems are based on two parts, the first involves designing the sliding surface allowing the sliding motion of the vehicle to satisfy with the design specification. The second concerning the control law selection attracting the switching surface to the system state. Sliding mode control presents two main advantages; firstly, allowing the dynamics of the vehicle to be tailored to the choice of sliding function. Secondly, some bounded disturbances, uncertainties and non-linearity become insensitive to the closed loop response allowing the controller to function smoothly.

7.2.4 Model Predictive Control

Model predictive control (MPC) aims to control multiple inputs and outputs simultaneously, whilst satisfying the input and output inequality constraints. This method uses a vehicle models current measurements to predict future output variables allowing appropriate changes to be made to achieve the desired behaviour. Model predictive control presents a few advantages:

- The control method is able to capture the static and dynamic interactions between output, input and disturbances.
- The constraints of these variables are taken into considerations using a systematic manner.
- The accurate predictions of the model can allow the prediction of potential problems in the vehicle.
  (Dale E. Seborg, 2010)

7.2.5 Model Reference Adaptive Control (MRAC)

MRAC's architecture includes an estimation of parameters to face the uncertainties of the vehicle system, a vehicle reference model to follow and an algorithm which modifies the control law, therefore, causing the vehicle to behave as desired. Running the adaptive algorithm and parameter estimation simultaneously results in direct MRAC, running separately results in indirect MRAC. This type of yaw rate control aims to ensure the robustness of the vehicle against the changes from the plant, caused by possible changes from external factors or variations in the parameters of the vehicle and provide a realistic scenario for the simulation. (Ghezzi, 2017)

7.2.6 Fuzzy Yaw Moment Control

Fuzzy yaw moment control introduces a non-linear method allowing controller to deal with complicated control problems. A fuzzy controller is constructed as a four-step system:

1. Fuzzification is the first step in this system and it alters the controller inputs so that, dimensionally they are compatible with conditions of knowledge-based rules by means of suitable linguistic variables.
2. The fuzzy decision process comes next, producing a fuzzy output by processing a rule list from the knowledge base and using the fuzzy input received in the fuzzification process.
3. Thirdly comes defuzzification. This step maps and scales the fuzzy output taken from the previous process, producing a value for the output. This output is the input of the actual system being controlled, in this case, it's the yaw moment.
4. The final process of fuzzy control is the output scaling. This process simply scales the controller output to map the preferred yaw moment.

This type of controller is widely used in applications where human operators are in control of the system. However, fuzzy yaw moment control is not a considerable controller when it comes to torque vectoring. (B. L. Boada, 2007)

7.2.6 Linear Parameter Varying Control

Linear parameter varying control systems are special types of non-linear systems due to their good suitability in controlling parameter varying dynamic systems. A systematic design procedure is provided using LPV techniques for multivariable gain-scheduled controllers.

This methodology allows the incorporation of bandwidth, performance and robustness limitations into a combined framework. (Stoop, 2014)

7.2.7 Yaw Rate Based Direct Yaw Moment Control

Yaw rate DYM methods considers the whole of the vehicles dynamics and aims to continuously control the yaw rate of the vehicle to achieve the dynamic behaviour desired. Typical controllers function using three set tasks:

1. Generation of a reference yaw rate.
2. Control algorithm (e.g. PID Controller).
3. Control actuation (Torque distribution to each individual wheel accordingly).

Each task can be approach through different methods producing different designs which can be effective in different scenarios.

A simple schematic of direct yaw moment control is presented in figure 7.1:

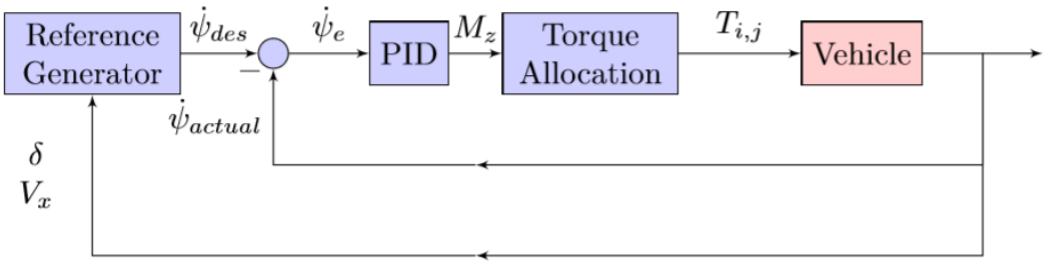

Figure 7.1: DYM Control (Vianna, 2018)

9. Control Strategy

This segment of the project covers the design of the control strategy employed into the vehicle system to improve the dynamic behaviour of it and increase the stability and control.

9.1 Preliminary Control

The preliminary testing for controlling the vehicle was compromised of a simple PID controller connected to an error value calculated through equation 9.1.2.

$$r_{ref} = k\delta \tag{9.1.1}$$

$$e = r_{ref} - r_{act} \tag{9.1.2}$$

The k value represented in the r_{ref} calculation represents a constant value necessary for the control of the yaw rate. The method for finding this k was to run the model without any active controller and monitor the steady state value and then run and monitor the steady state of the model using the control parameters, with $k = 1$, and finally dividing the steady state value of the inactive controller by that of the active controller to find the constant value which will allow the preliminary control of the system. The value found for k was 6.518. Once this value was set the system was simulated to monitor the yaw rate. In order to view the systems, control a separate constant can be introduced a changed. This value is labelled k_G and was altered from 0-2. Figure 9.1 shows the graph representing the change in yaw rate as the k_G is altered. The graph shows a linear increase in yaw rate proving the proof that the vehicle system can be controlled using a simple PID controller.

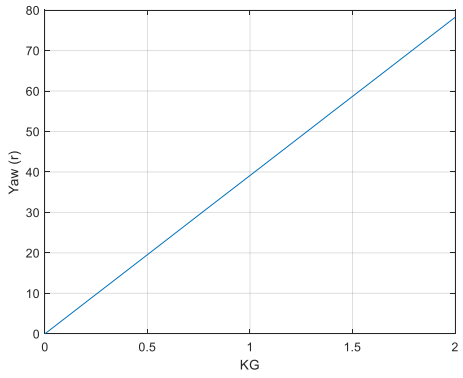

Figure 9.1: Preliminary Control

x	y
0	0
0.2	7.825
0.4	15.65
0.6	23.475
0.8	31.3
1	39.125
1.2	46.95
1.4	54.775
1.6	62.6
1.8	70.425
2	78.25

Table 1

Confirming the functionality of the preliminary controller allows the continuation of torque vectoring control by introducing a more complex strategy using the understeering gradient to control the yaw rate in a more accurate method.

9.2 Understeering Gradient

The understeering gradient plays an important role in the performance metric when analysing a vehicle's handling behaviour. It is known as the derivative of the average steering angle of the front wheel with respect to its lateral acceleration at the centre of gravity. This parameter can be measured by simulating a constant radius manoeuvre with a slow increase in longitudinal velocity, plotting lateral acceleration against the tyres steering angle. The

understeering gradient evaluates the tendency for a vehicle to understeer or oversteer when in a steady state curve manoeuvre.

Deriving an equation to calculate the reference yaw rate using the understeering gradient is as follows:

$$\delta = \delta_{dyn} + \frac{l}{R} \tag{9.2.1}$$

It is known that;

$$R = \frac{u}{r} \tag{9.2.2}$$

$$\delta_{dyn} = k_u a_y \tag{9.2.3}$$

$$\therefore \delta = k_u a_y + \frac{lr}{u} \tag{9.2.4}$$

The equation defining the lateral acceleration is also identified:

$$a_y = \dot{v} - ur \tag{9.2.5}$$

$$\text{at steady state } \dot{v} = 0 \therefore a_y = ur \tag{9.2.6}$$

$$\therefore \delta = k_u ur + \frac{lr}{u} \tag{9.2.7}$$

The understeering gradient, k_u, is defined through equation 9.2.8

$$k_u = \frac{d(\alpha_1 - \alpha_1)}{da_y} = \frac{d}{da_y}\left[\frac{ma_y}{l}\left(\frac{a_2}{c_2} - \frac{a_1}{c_1}\right)\right] \tag{9.2.8}$$

$$\therefore k_u = \frac{m}{l}\left(\frac{c_2 a_2 - c_1 a_1}{c_1 c_2}\right) \tag{9.2.9}$$

To clarify, the understeering gradient measures the change in difference between the trajectory curvature and the steering wheel angle. This difference is multiplied by constants in respect to the lateral acceleration. k_u is comprised of two terms, both are a ratio of the vertical load and the cornering stiffness acting upon each axle. Further analysis of equation 9.2.9 present three possibilities explained in the 'Fundamentals of vehicle dynamics' by T. D. Gillespie.

- When the vehicle is in a neutral steering position ($k_u = 0$), the steering wheel angle rate of change is proportional to the trajectory curvatures rate of change. There is no

required change in the steering wheel as the speed is varied. This causes a great balance between the cornering forces on both the front and rear so that the required steering angle will be equal to the kinematic steering angle $\delta = l/r$.

- At an understeering vehicle position ($k_u > 0$), the steering wheel angle rate of change is greater to the trajectory curvatures rate of change. In this case the front two wheels have a greater slip than the rear two and when keeping the cornering radius the same, increasing the speed should lead to an increase in the steering wheel angle. This causes stable behaviour which is why many vehicles are designed using understeering characteristics in compromise of slower response time.
- The reverse of this occours when the vehicle is oversteering ($k_u < 0$). This is when there should be a decrease in steering angle when the lateral acceleration or speed is increased causing a larger slip angle on the rear two wheels producing a reduction in the radius of cornering from the outward drift. This unstable behaviour will continue till the steering wheel angle is reduced in order to maintain the radius of the curve.

The change in steering wheel angle with speed, maintaining a constant cornering radius and lateral acceleration is present in figure 9.2**.** The characteristics presented in this graph are derived using steady state conditions, however, the results can be applied for other scenarios to analyse a vehicles response and its handling. The character speed is the speed where the kinematic steering angle is half the actual steering angle. The figure shows in a neutral steer the steering angle (δ) remains constant. An understeering vehicle has an angle which increases with square of speed until it reaches the characteristic speed. An oversteering scenario causes the steering angle to decrease with the speed squared until it reaches critical speed to which it becomes 0.

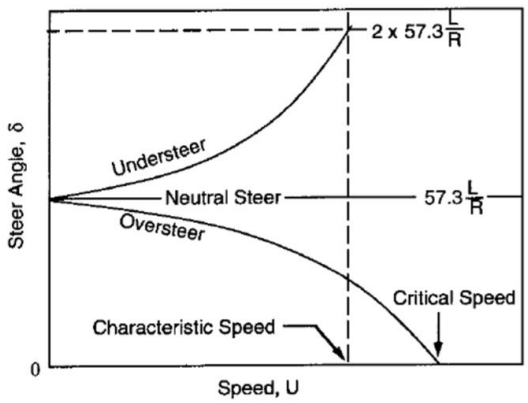

Figure 9.2: Change of steer angle with speed (Gillespie, 1992)

Rearranging equation 9.2.7 allows the calculation of the reference yaw needed to calculate the effort value:

$$r_{ref} = \frac{\delta u}{k_u u^2 + l} \tag{9.2.10}$$

Substituting the understeering gradient equation into equation 9.2.10 gives the final equation submitted to Simulink giving the final reference yaw rate equation

$$r_{ref} = \frac{\delta u}{\frac{m}{l}\left(\frac{c_2 a_2 - c_1 a_1}{c_1 c_2}\right) u^2 + l} \tag{9.2.11}$$

This yaw rate reference is a grain representing how much the yaw rate is increased in accordance to the steering input. Figure 9.3 represents a graph comparing the behaviour of the different type of steering plotting speed against the yaw velocity gain. Monitoring the neutral steer shows a linear relationship between the speed and yaw rate gain. Understeering a vehicle causes an increase in yaw velocity gain until it reaches characteristic speed which it then begins to decrease. Finally, an oversteering car will result in the yaw rate velocity becoming infinite at critical speed. (Gillespie, 1992)

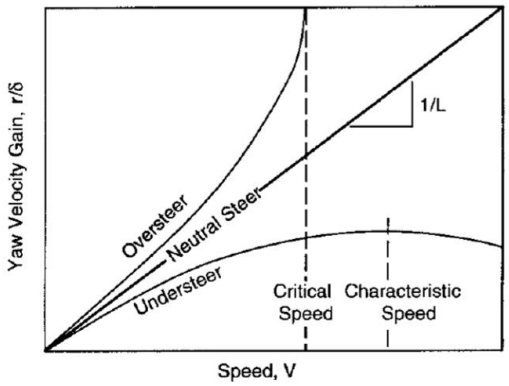

Figure 9.3: Yaw velocity gain as a function of speed (Gillespie, 1992)

The understeering gradient (k_u) is a fundamental expression in controlling the yaw rate of a vehicle to reach a desired value and the expression is fundamental when developing this type of yaw rate controller.

10. Input Signals

The steering angle contributes a fundamental role in the several components of the system. It is necessary to calculate the lateral forces, the moments, the torque vectoring algorithm hence the desired yaw rate. The steering angle is designed as an input parameter permitting the simulation of real-life scenarios through alteration of the input curvature using different sink blocks in the Simulink library. The manoeuvres which were simulated to find the results were:

- Step – A step creates a simplistic nonlinear, steep shape providing an unrealistic scenario of a vehicle manoeuvre. However, it helps considerably with understanding the vehicles dynamic behaviour. The step response allows the ease of studying the control performance when considering the settling time, overshooting, unstable zones and identifying any oscillations.
- Ramp – Still far from creating a realistic manoeuvre, a ramp simulates a softer scenario by presenting a discontinuous change in slope, still corresponding to the desired position of the steering wheel but taking a longer time to reach that desired value.
- Single Lane Change – This is one of the most common ISO standard vehicle simulations used when testing a vehicles functionality. A single lane change manoeuvre provides a variety of real-life situations such as driving on a motorway, overtaking or a sudden avoidance movement.
- Double Lane Change – Following the similarity of the single lane change, the double lane change simply includes an extra pulsation with the opposite sign to the first, maintaining a steering angle of zero in between the movement. A schematic of the ISO double lane change manoeuvre is provided in figure 10.2.
  (Ghezzi, 2017)

Figure 10.1 presents the curvature of these manoeuvres as graphs simulated in Simulink.

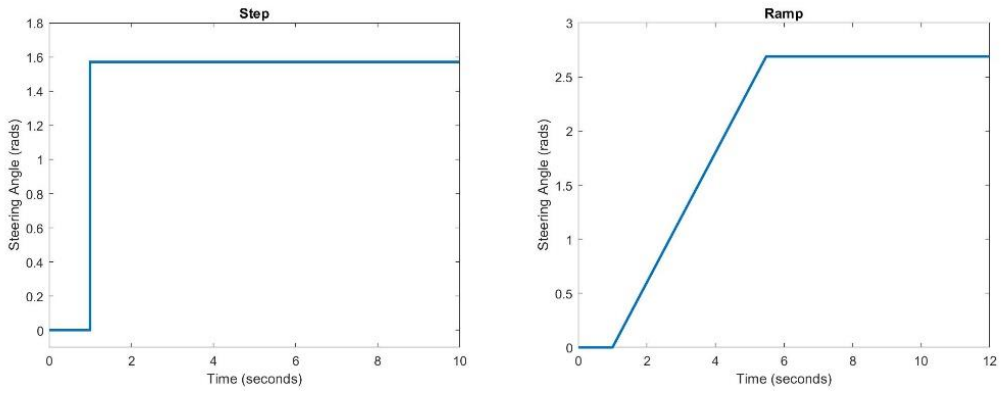

a) Step Response *b) Ramp Response*

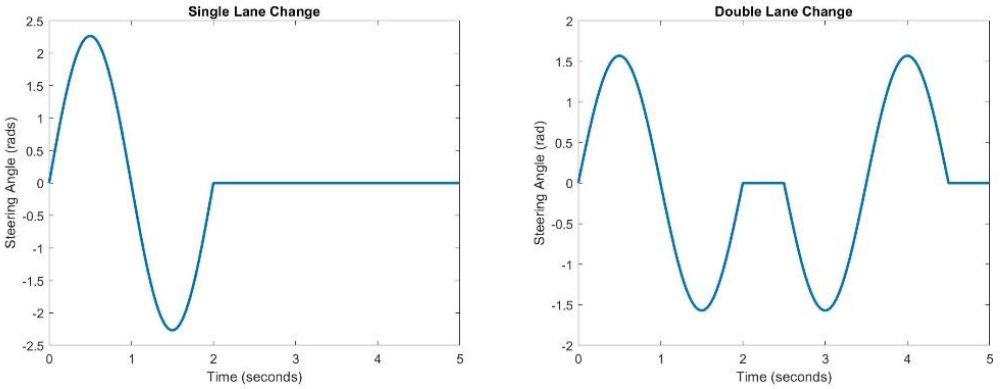

c) Single Lane Change *d) Double Lane Change*

Figure 10.1: Input Signals

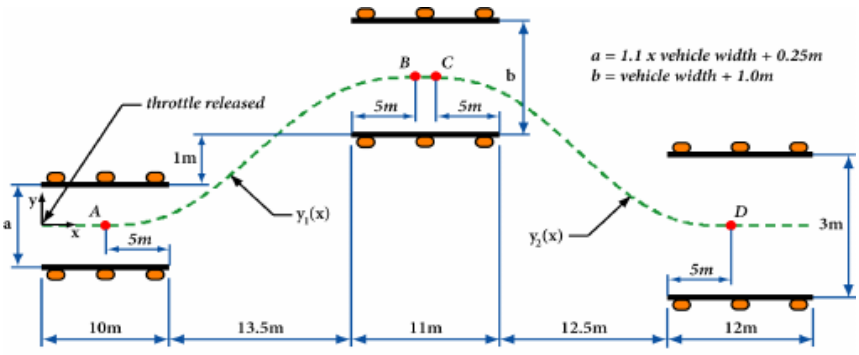

Figure 10.2: ISO Double Lane Change (Kiumars Jalali, 2013)

11. Simulation and Analysis of the Results

This part of report provides the results of the simulation of the complete torque vectoring control strategy, designed in previous sections, along with the description of the behaviour of each monitored parameter under specific input conditions. The results show the efficiency and the effectiveness of the designed active torque vectoring system in comparison to a passive vehicle model when attempting to follow the reference value gained using the understeering gradient (section 9.2). All simulations are approximated reproductions, simplified from real life scenarios. Although these results do not provide the most accurate set of data, it does however, give an accurate representation of the behavioural dynamics of an electric vehicle.

11.1 Step Response

The step response simulation was completed using a maintained longitudinal velocity of 25m/s and step input steering angles of $\pm 50°, \pm 90°$ and $\pm 130°$ at a step time of $1s$ into the simulation.

The first case scenario presents the unrealistic step response of the controller, however, still providing a significant evaluative control performance. Figure 11.1 shows the simulation results for each inputted steering angle, tracking of the passive yaw rate of the vehicle (green), active yaw rate (red) beside the value for the reference yaw rate (blue). The passive vehicle controller reaches its steady state value after approximately $2s$ into the simulation, however, the final value $(39.73\ deg/s)$ for this controller is significantly larger than the desired reference value of $25.2\ deg/s$. The active yaw rate controller, on the other hand, reaches the desired steady state condition of $25.2\ deg/s$ after approximately $6s$ into the simulation. The initial overshoot peak produces a 13.16% error prior to settling to its steady state value. This over shoot error could be altered by reducing he integral gain at the cost of a longer settling time. The presence of errors in this simulation is acceptable due to the step manoeuvre being unable to represent a real-life situation.

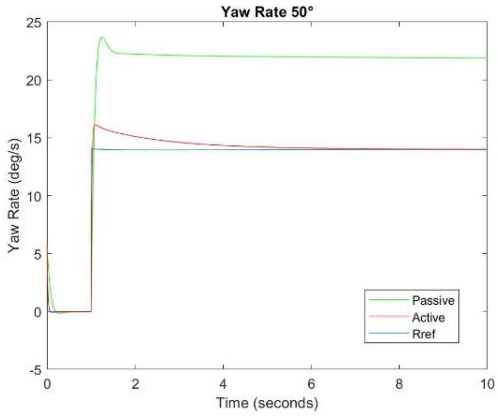

a) 50° Steering Angle

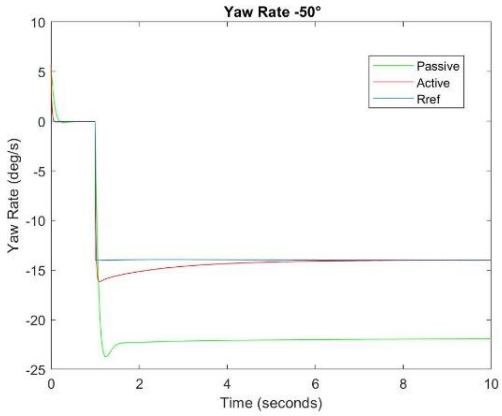

b) -50° Steering Angle

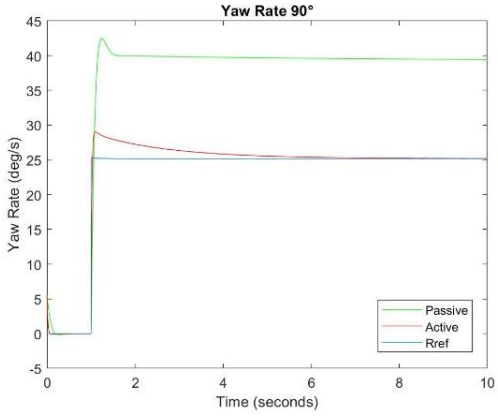

c) 90° Steering Angle

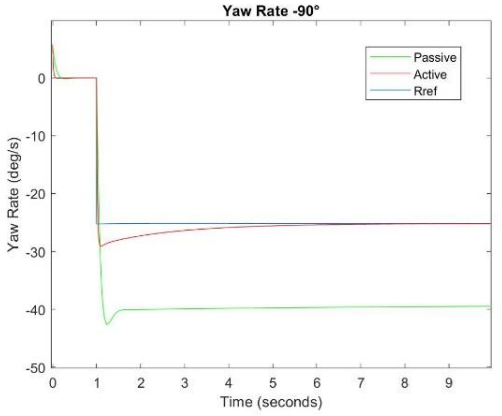

d) -90° Steering Angle

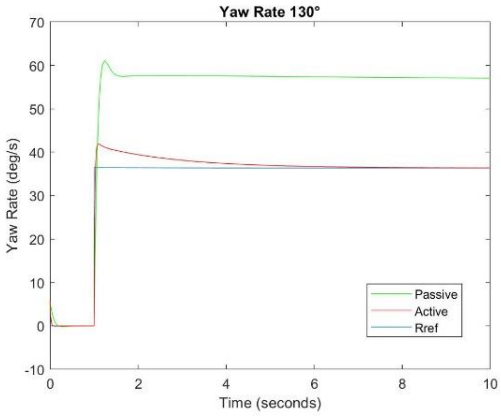

e) 130° Steering Angle

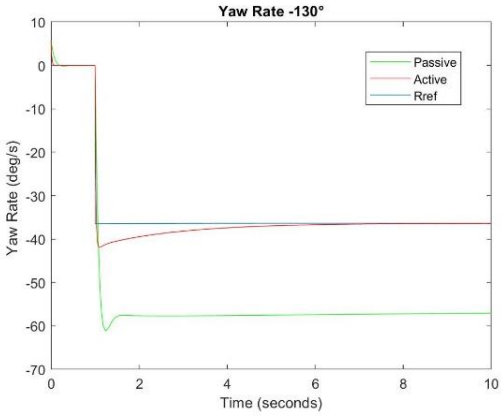

f) 130° Steering Angle

Figure 11.1: Step Response Yaw Rates

11.2 Ramp Response

The discontinuous change in slope shown in figure 10.1 was completed by using a ramp input, allowing the increase of steering angle, followed by a saturation block, giving the system its final steering angle. The system was simulated in two methods; the first was a constant increase in the steering angle from $0°$ to $+130°$, the second being the opposite and simulating a constant decrease in the steering angle from $0°$ to $-130°$.

The simulation results with the ramp input are presented in figure 11.2. Again, the graphs show the tracking of the passive yaw rate of the vehicle (green), active yaw rate (red) beside the value for the reference yaw rate (blue). The results show a similar scenario to that of the step input in that the passive vehicle controller presents a large 36.19% error when trying to control the yaw rate to the desired reference values. In contrast, the active yaw rate control is able to track closely the desired reference yaw rate corresponding with a 3.01% error at its maximum peak.

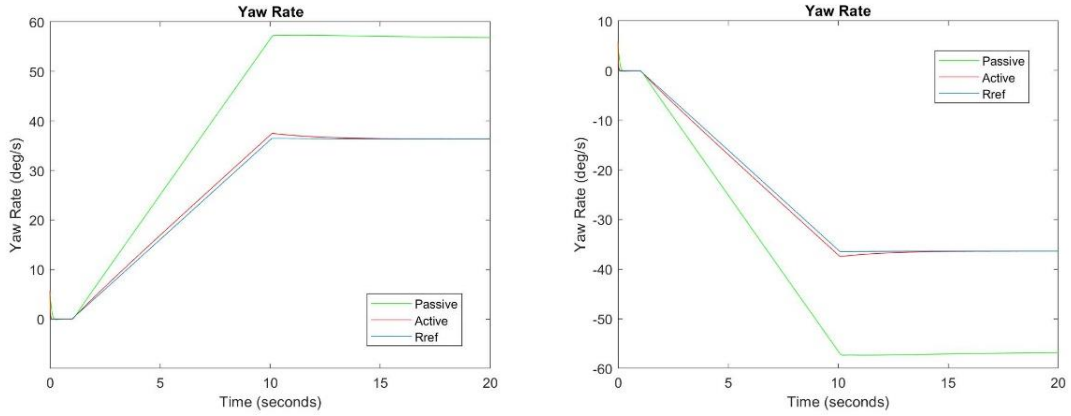

a) Positive Steering Angle *b) Negative Steering Angle*

Figure 11.2: Ramp Response Yaw Rate

11.3 Single Lane Change

The single lane change is a complicated manoeuvre to simulate. The method, which was taken to achieve this manoeuvre, presented in figure 10.1**,** the frequency of sine waves outputted from the sing input block would need to be reduced to one. This was completed by subtracting a sine graph, saturated so that it begins at $2s$, from the sine input block, therefore, removing all sine waves after the initial one. The system was then simulated using three different steering angles; $50°$, $90°$ and $130°$.

The colour scheme in figure 11.3 has the same legend as the previous simulations where the tracking of the passive yaw rate of the vehicle (green), active yaw rate (red) beside the value for the reference yaw rate (blue). The results of the passive vehicle control simulation once again presented errors when attempting to follow the reference yaw rate resulting in a 38.11% error at its peak. However, under the conditions of an active yaw rate controller, the system becomes significantly more accurate when tracking the reference, resulting in a peak 13.24% error in the simulation.

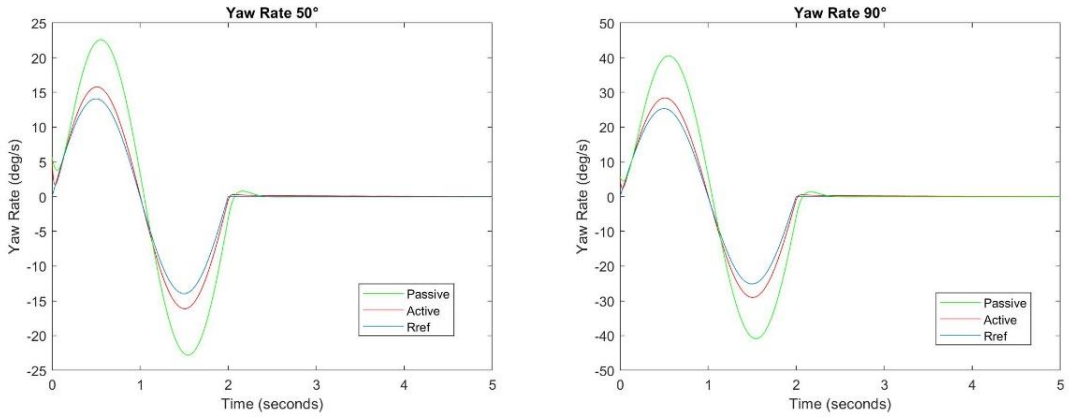

a) 50° Steering Angle

b) 90° Steering Angle

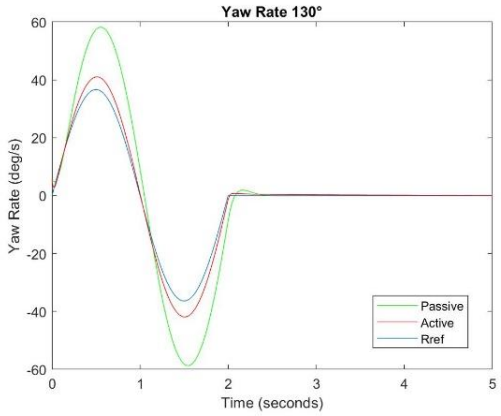

c) 130° Steering Angle

Figure 11.3: Single Land Change Yaw Rate

11.4 Double Lane Change

The complication of the single lane change manoeuvre is amplified when attempting to simulate the double lane change manoeuvre. The Simulink simulation consisted of the subtraction of certain sections of the sine wave, using saturated sine blocks whilst adding a reversed saturated sine wave, giving the system an initial sine wave, a 0.5s break followed by a single reversed sine wave. Figure 11.4 shows the results of this simulation.

The results present similarity to the single lane change simulation. Once again, the passive vehicle control system (green) struggles to maintain the desired yaw rate when tracking the reference yaw rate, producing a 38.27% error at its highest peak. Alternatively, the controlled active vehicle model manages to track the reference yaw rate closely producing a minimalistic 13.57% error at its highest point.

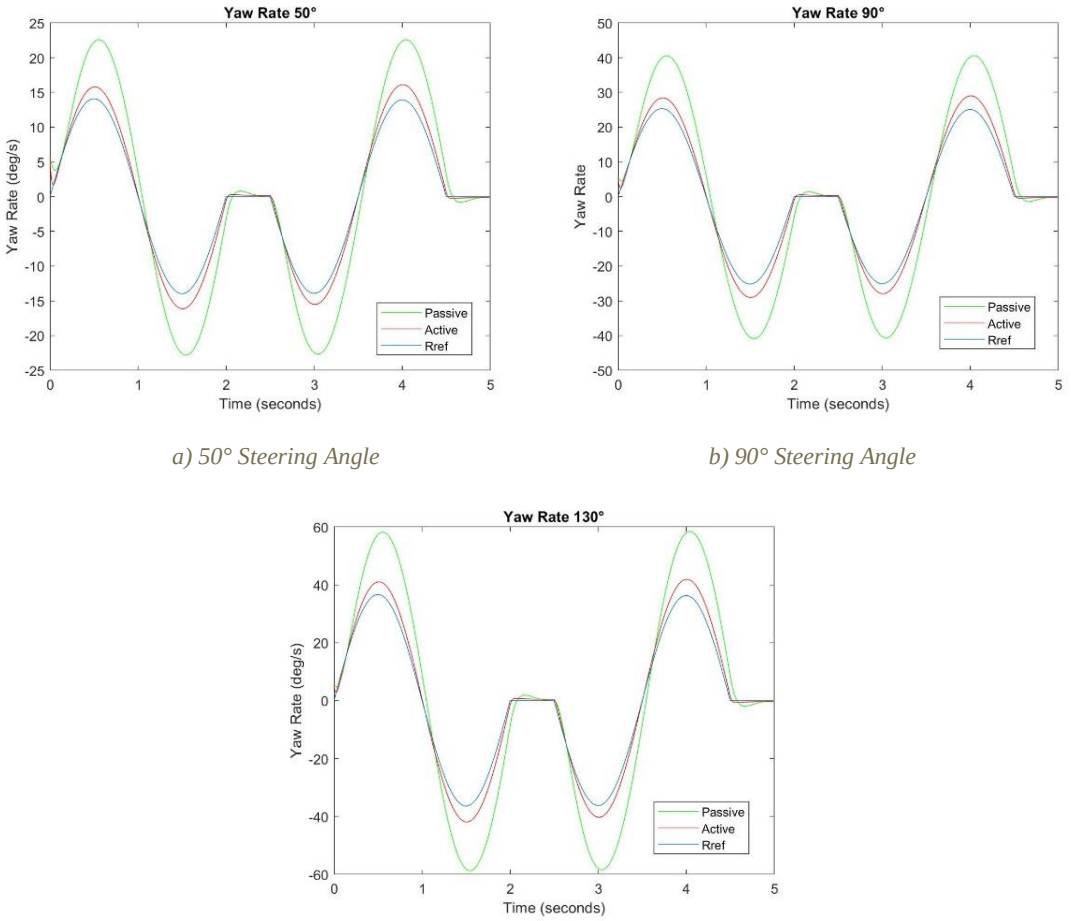

a) 50° Steering Angle

b) 90° Steering Angle

c) 130° Steering Angle

Figure 11.4: Double Lane Change Yaw Rate

11.5 Control Strategy: Conclusion

Considering the several test procedures, it is evident that the designed torque vectoring controller has a significant effect in the vehicle's dynamic behaviour. When using this controller, the lateral behaviour improves significantly, leading to the capability of reaching higher velocities when cornering, whilst keeping the vehicles stability. In summary, the results achieved presented accurate enough data to consider the designed system as a function torque vectoring controller. The more reliable simulations included the single lane change and double lane change as they simulate real life scenarios according to ISO standards. The designed close look system is stable, and the tracking of both the lateral velocity and yaw rate are acceptable. These simulations showed a maximum error of 13.57% which is relatively low for the designed torque vectoring system showing promising results. The PID controller provided an increase in lateral performance and capability of controlling the yaw rate compared to the vehicle model without torque vectoring. However, with a deeper and more comprehensive vehicle model, the dynamic behaviour can be simulated with greater accuracy and reliability.

12. Comparison

In this section the designed torque vectoring controller will be compared to other designed controllers using several different techniques to control the yaw rate of a vehicle. The torque vectoring method used in these controllers are explained in section 7.2. The designed systems in other papers contain more thorough research and have access to more advanced technology and resources allowing them to design are more capable controller. However, the controller designed in this report can still be used to compare the tests and hence look for improvements to achieve better yaw rate control.

12.1 Sliding Mode Control (SMC)

The first set of compared results, completed by Matteo Kevin Ghezzi, are based upon sliding mode control. The system, explained previously, is tested using the same standard manoeuvres as the designed torque vectoring controller, excluding the ramp response. However, the simulations are run using the same steering angle $(90°)$ and constant longitudinal velocity $(60km/h = 16.6m/s)$. The results for each manoeuvre are presented in figure 12.1.

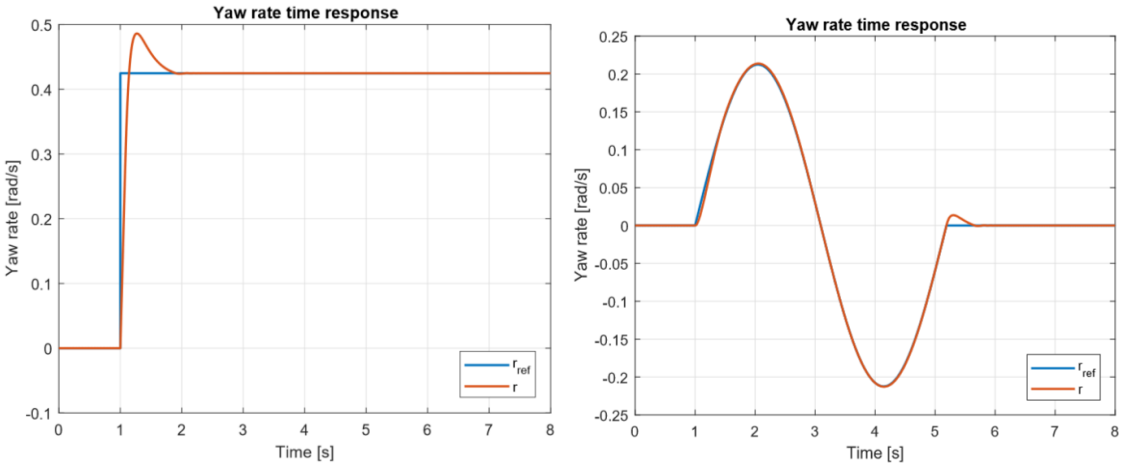

a) Step Response *b) Single Lane Change*

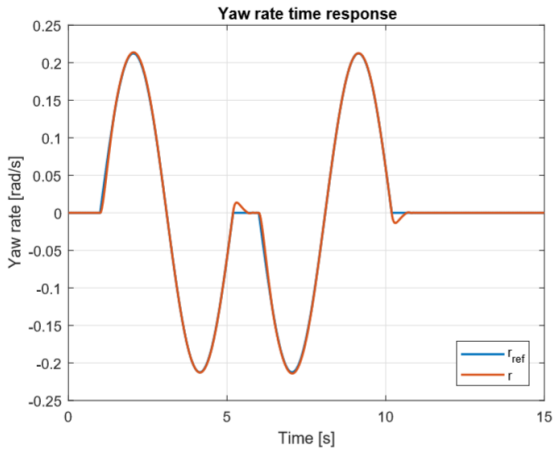

c) Double Lane Change

Figure 12.1: SMC Results (Ghezzi, 2017)

The first case analysis is in response to the step input. As can be seen, the actual yaw rate (red) reaches a steady state value after approximately $1.4s$, producing a 14% overshoot peak.

Comparing this result to the designed PID torque vectoring controller provides a slightly better overshoot peak of only 13.16%, however, this is in compromise of a longer settling time of $6s$. As stated previously, this settling time can be reduced by increasing the integral gain in compromise of a larger percentage overshoot.

The next two simulations carried out by the sliding mode controller were the single and double lane change. Both these simulations produce similar accuracy, essentially due to them being the same manoeuvre but repeated in the opposite direction. The simulations proved good tracking of the reference yaw rate, producing a maximum overshoot delay of $6s$ and an error of $1.8 \times 10^{-2}\ ras/s$, at the end of each manoeuvre. This is due to the cause of the control law; therefore, it is inevitable. In comparison to the simulation carried out by the designed torque vectoring system, the SMC yaw rate controller proved significantly more effective when following a referenced yaw rate.

Concluding the sliding mode controller results signified it to be more effective and efficient, in terms of controlling the yaw rate. The controller designed by Matteo Kevin Ghezzi is designed using a considerable amount of extra resources and a more in-depth study into the vehicle dynamics producing a more accurate and effective torque vectoring controller.

12.2 Mode Reference Adaptive Control

The second set of reviewed simulations were carried out using the MRAC method, completed also Matteo Kevin Ghezzi using the same parameters as previously. Figure 12.2 presents the results for the simulations completed in the thesis.

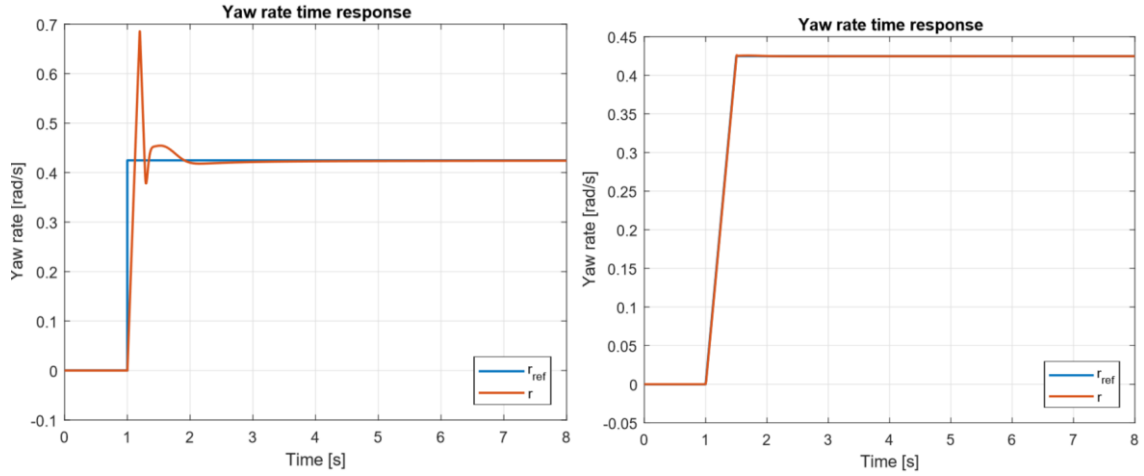

a) Step Response *b) Ramp Response*

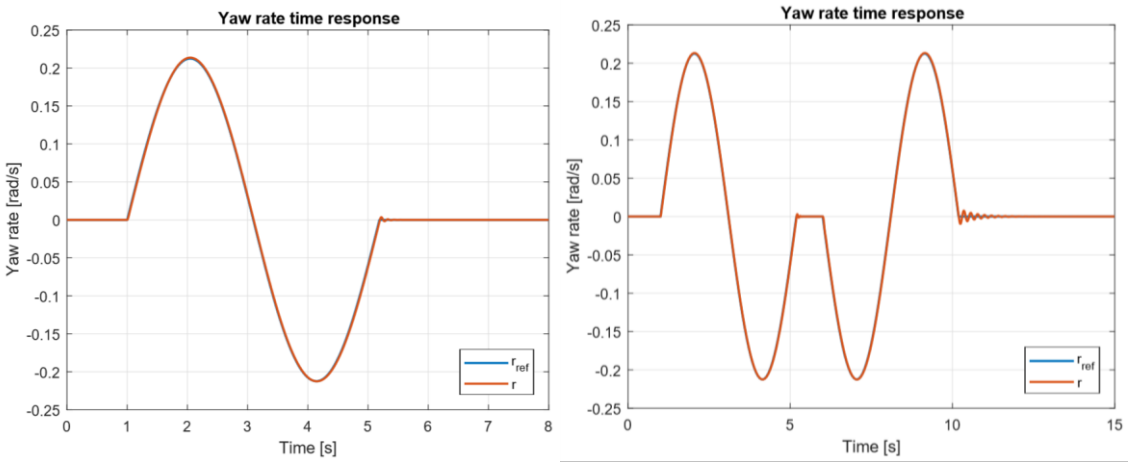

c) Single Lane Change *c) Double Lane Change*

Figure 12.2: MRAC Results (Ghezzi, 2017)

The first analysed case of this control method is using the step response, a**.** the graph clearly shows the tracking ability for the MRAC to be very poor in terms of a step response, due to the very large percentage overshoot and the oscillation up until it reached its final value. However, due to the unrealistic manoeuvre that the step response is, this data does not define the whole system.

Looking towards the three next simulations, which included the ramp response, single lane changes and double lane change, the accuracy of the system increased significantly. With the ramp as an input the system is capable of tracking the reference yaw rate with only a 2.6% error at its highest peak. In consideration of the single lane change manoeuvre, the system isn't capable of achieving the same accuracy, however, despite experiencing a small amount of chattering ($0.015\ rad/s$ at the maximum) then the movement is complete. The same situation occurs when simulating the double lane change except the oscillation is greater and persists for a longer period during the second change. The accuracy of these manoeuvres seemed to be significantly high in terms of tracking the reference yaw rate proving the MRAC to be effective in more realistic scenarios.

Comparing these simulations with the designed controller shows the MRAC to be more effective with the more realistic manoeuvres, furthermore, the designed controller is able to closely control the error once the manoeuvre is over, removing any undesired oscillation.

12.3 PID controller

The next set of compared data was from a previously designed model of a PID yaw rate controller, finding a reference value using the understeering gradient, similar to the one designed in this report. The controller and results were designed and found from a master's degree thesis 'Torque Vectoring in Electric Vehicles with In-wheel Motors' by Joao Pedro Almeida Vianna. The results which are going to be analysed are all completed using a constant speed of $120km/h$ $(33.33m/s)$ and a steering angle of 6 degrees. The two manoeuvred results from the report was the step steer and the double lane change presented in figure 12.3.

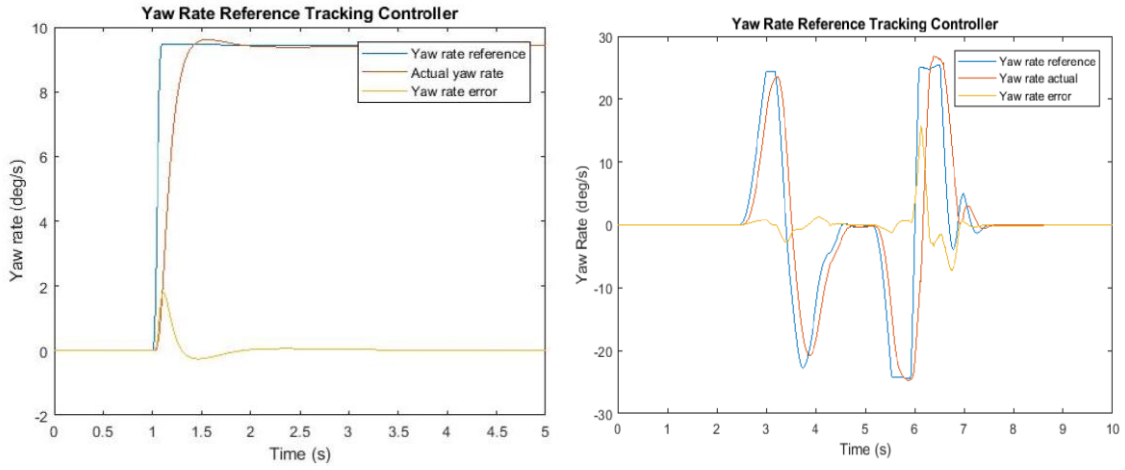

a) Step Response *b) Double Lane Change*

Figure 12.3: PID Controller Results (Vianna, 2018)

Analysing the trackinng of step response simulation shows the system achieves a steady state value after aproximately $0.7s$ producing a overshoot error of 2% as can be seen from the yaw rate error. In contrast to the designed PID torque vectoring controller the error of the system is significantly lower to the 13.16% received by the deigned controller along with the improved settling time of $0.7s$ weighed up to the $6s$ needed for the designed controller. The possible resasons for this significant difference in the control accuracy are the increased calculations and equations used to create the vehicle model and controller, therefore producing more reliable results and estra parameters to help the tracking of the referance yaw rate.

The second scenario simulated the ISO standard double lane change. The simulation is able to closely control the yaw rate in accordance to the referance yaw rate, however, the accuracy of the data decreases as the simulation is run through the $10s$ reaching a maximum error of aproximately 15% which is slightly higher than the error achieved from the designed controller. The accuracy in completing a more realstic manouver was greater in the designed PID controller than the controller from the paper by Joao Pedro Almeida Vianna. The designed PID controller was capable to control the yaw rate in the double lane change keeping the error almost constant throughout the whole $10s$ simulation.

In summary, comparing the two controllers prove that using a PID controller to control the yaw rate of the system gives similar accuracy in tracking a reference. Both controllers are successful in altering the vehicle response and helping the vehicle reach a steady state.

12.4 Linear Parameter Varying Controller

In the master thesis ‘The design and implementation of torque vectoring for the forze facing car’ by Anton Stoop follows the design of a linear parameter varying controller. The controller simulation is carried out using a constant lateral velocity of $60km/h$ $(16.67m/s)$ with an initial step input of $30°$ carrying out the step response manoeuvre. Figure 12.4 presents the results of this simulation.

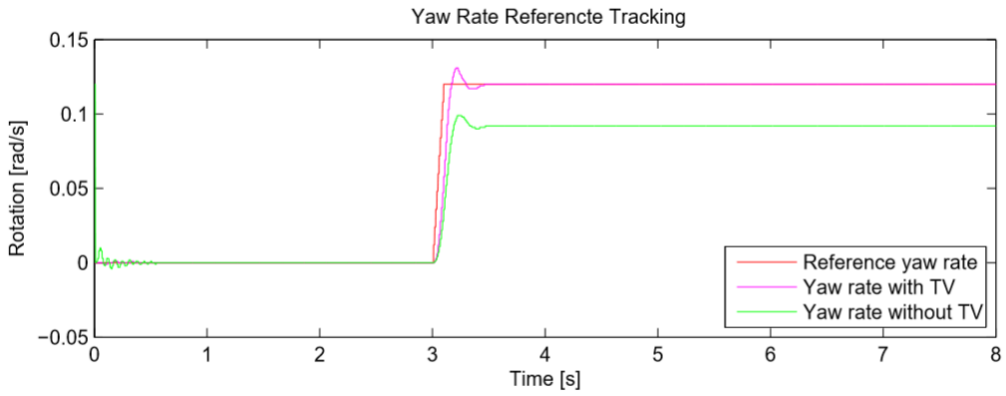

Figure 12.4: Step Response LPVC Results (Stoop, 2014)

The step response manoeuvre shows the LPC controllers' capability of following the reference yaw rate is very efficient. The system reaches its steady state value after approximately $0.26s$ after the steer input, producing an overshoot of 9.2%. The torque vectoring capability of this controller is the most effective out of all the controllers compared so far in terms of the step response manoeuvre. Therefore, in comparison to the designed controller, the LPC controller produces a more accurate yaw control. The LPC controller simulates other types of standard manoeuvres which means they are difficult to compare because of their differences.

12.5 Comparison: Conclusion

In summary, the designed controller which uses the understeering gradient to find a reference yaw rate, compared fairly well against previously designed controllers considering the details in the design of the vehicle model and the controller. The several types of yaw rate control methods all proved to be effective and efficient in their own way, resulting in different methods being more desirable when carrying specific needs than others. Improving the torque vectoring controller, which was designed, through methods explained further on in the report, could possible increase the accuracy and reliability of the simulations and a more detailed comparison can be made.

13. Conclusion

The aim of this project was to design a mathematical four-wheel drive vehicle model and implement a torque vectoring controller to control the yaw rate and access its performance capabilities.

The mathematical vehicle model was created using Simulink and MATLAB through the integration of a series of equations deriving the vehicle. The programming simulates a double track all-wheel drive vehicle model based upon rigid bodies, to derive the framework, and tyre models, to derive the forces acting on the system. The torque vectoring controller was designed to exploit the many possible advantages of introducing individual electric motors on each wheel through a yaw rate-based approach aiming to increase the stability and control of the car under several steering conditions and manoeuvres.

Demonstrated in section 11 of this report, the controller is capable of successfully changing the vehicles response, therefore increasing the comfort for the driver. During all manoeuvres, the controller is able to track the reference yaw rate of the vehicle closely producing minimalistic error. Comparing the model to other designed controllers using several different methods proved the system to fare well against them when considering the complexity of the design and the resources provides. However, there is still room for significant improvements in the system which are discussed in the next section.

14. Future Work

Although the torque vectoring system, proved to be effective in controlling the yaw rate, there is still some major improvements that could be made to increase the accuracy, efficiency and reliability of the system when considering real life scenarios. In order to find future work that could possibly expand and improve the TV system, it is a good idea to look at pre-existing torque vectoring models.

14.1 Vehicle Model

The vehicle model designed in this project proved sufficient in its job of simulating real life actions of a four-wheel drive system. However, the systems complexity was minimal compared to other thesis' due to the implementation of several extra parameters and variable to improve the accuracy of the model. The system is designed to run on a flat surface therefore limiting the realism of a real-life road. Introducing equations which take into account the road surface and incline the model's reliability will increase significantly. This could also include introducing a suspension system to measure the osculation of the spring and consequently the stability of the vehicle. The other method is to introduce more resistive aspects to the vehicle such as rolling resistance and hill climbing force to take the realism of the model even further.

14.2 Control Methods

The comparison section of this project presented many different methods of torque vectoring, each presenting their advantages and disadvantages when aiming to increase the stability of the vehicle. Improving this project could be completed through the integration and testing of the several types of torque vectoring controllers on the same vehicle model to monitor the quality of control from each method.

14.3 Monitorisation of the torque

Master thesis papers such as 'Control of a Four In-Wheel Motor Drive Electric Vehicle' by Matteo Kevin Ghezzi have designed vehicle models capable of monitoring the torque distribution in the vehicle. This function can largely increase the desirability of the system as it presents valuable information about the control of the vehicle. (Ghezzi, 2017)

14.4 Physical Validation

As stated previously, the system does not obey all the laws of an actual vehicle model, to which other aspects could be introduced to increase the realism of the system. If this improvement was to prove successful, future work could include the implementation of the torque vectoring controller onto an actual vehicle. All the systems testing in this repost are virtual and theoretical therefore in order to validate the results, the system would need to be integrated onto a fully functional vehicle with four individually controller motors.

15. Critique

The main aim of this project was to design and implement a vehicle model and a torque vectoring controller using MATLAB and Simulink to enhance the driving stability and safety without compromising the users driving experience. This report includes a fully functional mathematically modelled double track model and a torque vectoring controller applied onto it which effectively was able to control the yaw rate of the vehicle, therefore, improving the driving stability and safety. Some of the aspects discussed in section 14, such as the addition of the rolling resistance and hill climbing force, could not be included in the project due to time restrictions and workload, even though this would have increased the reliability of the designed system.

At the beginning of the project a Gantt chart was designed to provide an efficient and effective method to complete the project on time and with a high quality, see appendix. The final year of university studying mechanical engineering proved a tough task due to many assignments and exams taking up a lot of time throughout the year and causing this project to be set aside at certain periods of this final year. However, due to effective time management and organisation each task in the project was kept on or ahead of track in accordance to the Gantt chart, with the help of regular scheduled meetings with Dr Basilio Lenzo to ensure the project was progressing.

16. Personal Reflection

Starting this project with only a brief understanding of what torque vectoring is allowed a successful, in depth and thorough research to be carried out in order to understand the concept and the possibilities of the vehicle dynamic control it comes with. The project title of torque vectoring in electric vehicles opened many methods to approach the topic, therefore, guiding me to approach the project using an engineering mindset in order to complete and achieve the aims of this project. With the guidance of my supervisor, Dr Basilio Lenzo, and the use of many reliable sources, referenced in the bibliography, my familiarity of mathematical modelling, vehicle dynamics and yaw rate control strategies were broadened significantly giving me the capability and knowledge necessary when designing the vehicle model and torque vectoring controller.

The key success factor in the completion of this project comes largely down to the design of a successful, fully functioning mathematical vehicle model. Entering this project with a strong mathematical background supported the understanding of each equation deriving the double track, allowed a quick and effective completion of a vehicle model forming the groundwork for the whole project.

If I was to carry out this project again the changes, I would dedicate more of my free time into it so that more aspects mentioned in section 14 can be completed increasing the accuracy and reliability of the results gained. Another possibility of improving this project is to extend the literature review and research in order to increase the knowledge and understanding of torque vectoring therefore increasing my capability of the designing the controller.

Overall, the project has challenged my engineering capabilities and has helped me to improve as an engineer giving me valuable skills I can used in the future. The project has been very interesting and enjoyable and has given me a desire to hopefully pursue a career in this sector of engineering.

17. Bibliography

1. Anderson, R. H. (2011). *Dynamics of Vehicles With In-wheel Motors.* Cambridge: Cambridge University.
2. B. L. Boada, M. J. (2007). *Fuzzy-logic applied to yaw moment control for vehicle stability.* Taylor & Francis Online.
3. Belisso. (2009). *Torque Vectoring: side-to-side torque transfer technology*. Retrieved from Torque Vectoring Technology.
4. Chan, C. (2002). *The state of the art of electric and hybrid vehicles.* Beijing: IEE Explore.
5. Collins, D. (2019, April 11). *How Car Steering Systems Work*. Retrieved from CarBibles: https://www.carbibles.com/car-steering-systems/
6. Dale E. Seborg, D. A. (2010). *Process Dynamics and Control.* John Wiley & Sons.
7. Fu, C. (2014). *Direct Yaw Moment Control for Electric Vehicles with Independent Motors.* Melbourne: RIMIT University.
8. Gan, Y. H. (2013). *A Torque Vectoring Control System for Maneuverability Improvement of 4WD EV.* Scientific.Net.
9. Ghezzi, M. K. (2017). *Control of a Four In-Wheel Motor Drive Electric Vehicle.* Barcelona: Polytechnic University of Catalonia.
10. Gillespie, T. D. (1992). *Fundimentals of Vehicle Dynamics.* Society of Automotive Engineers.
11. Guiggiani, M. (2014). *The science of vehicle dynamics handling, braking, and ride of road and race cars* . England: Dordrecht : Springer.
12. Hall, N. (2015, May 05). *Aircraft Rotations -Body Axes*. Retrieved from National Aeronautics and Space Administration: https://www.grc.nasa.gov/WWW/K-12/airplane/rotations.html
13. Kaiser, G. (2015). *Torque Vectoring - Linear Parameter-Varying Control for an Electric Vehicle.* Hamburg: Technical University Hamburg.
14. Kiumars Jalali, T. U. (2013). *Development of an Advanced Fuzzy Active Steering Controller and a Novel Method to Tune the Fuzzy Controller* . Waterloo: SAE International .
15. Kou, F. G. (2010). *Automatic Control Systems.* Versailles: John Wiley & Sons.
16. MicheleVignati. (2016). *Innovative Control Strategies For 4wd Hybrid and Electric Vehicles.* Milano: POLITECNICO DI MILANO.
17. PistonPuff. (2017, October 25). *What is a Steering Ratio, Gear Ratio and Variable Gear Ratio in a Rack & Pinion type automotive steering system?* Retrieved from PistonPuff: http://www.pistonpuff.com/what-is-a-pinion-in-a-rack-pinion-type-automotive-manual-steering-system/

18. Sena TEMEL, S. Y. (2015). *P, PD, PI, PID CONTROLLERS* . MIDDLE EAST TECHNICAL UNIVERSITY .

19. Stoop, A. (2014). *Design and Implementation of Torque Vectoring for the Forze Racing Car.* Delft: Delft University of Technology.

20. Vianna, J. P. (2018). *Torque Vectoring in Electric Vehicles with In-wheel Motors.* Torino: Polyethnic of Torino.

21. Vos, R. (2010). *Influenceofin-wheelmotorson theridecomfortofelectricvehicles.* Eindhoven : Eindhoven University of Technology .

22. *What is Torque Vectoring?* (n.d.). Retrieved from Torque Addict: http://torqueaddict.com/what-is-torque-vectoring/

18. Appendix

18.1 Single Track Model

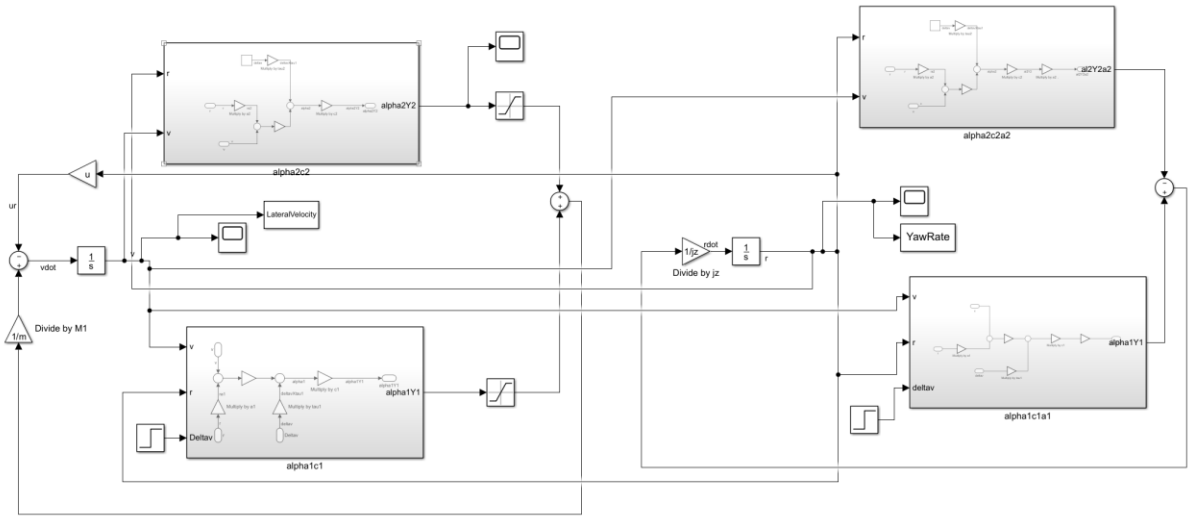

Figure 18.1: Single Track Model

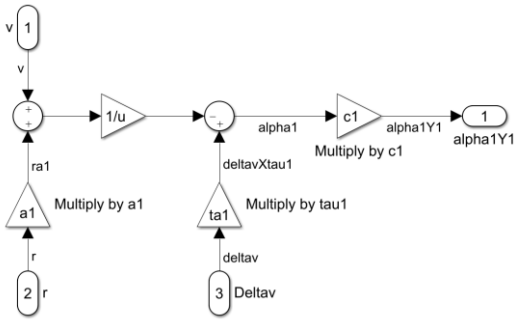

Figure 18.2: $\alpha_1 C_1$

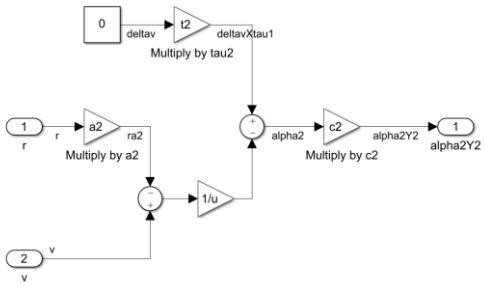

Figure 18.3:$\alpha_2 C_2$

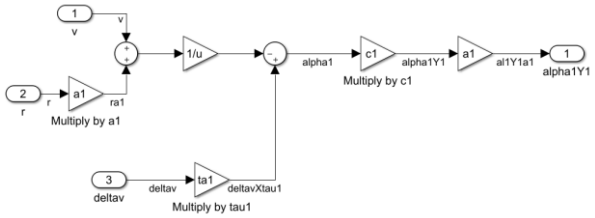

Figure 18.4: $\alpha_1 C_1 a_1$

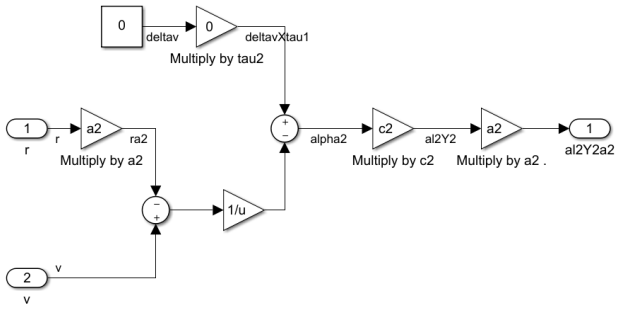

Figure 18.5: $\alpha_2 C_2 a_2$

18.2 Double Track Model

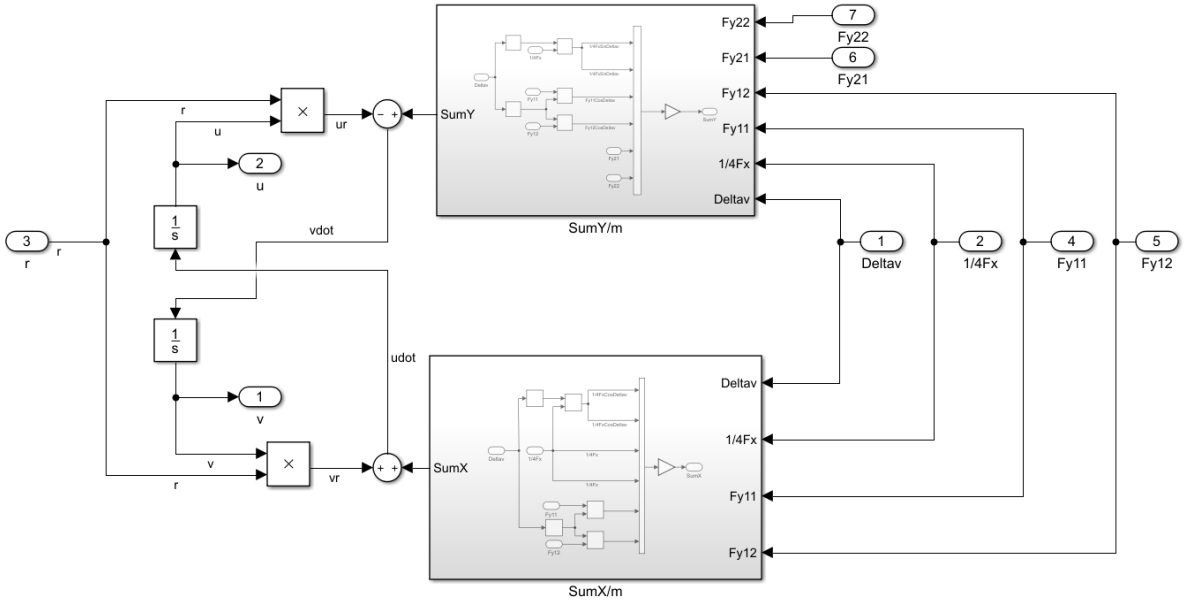

Figure 18.6: Lateral and Longitudinal Forces

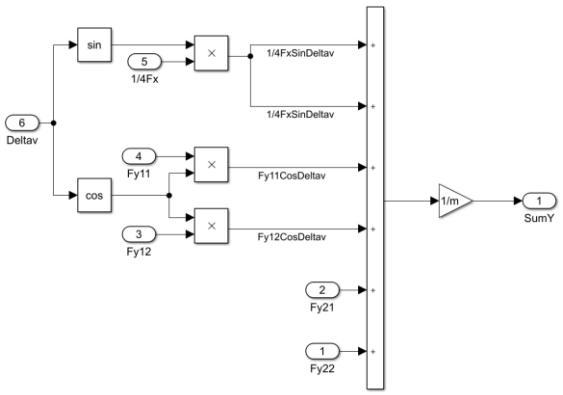

Figure 18.7: Sum of the longitudinal forces over m

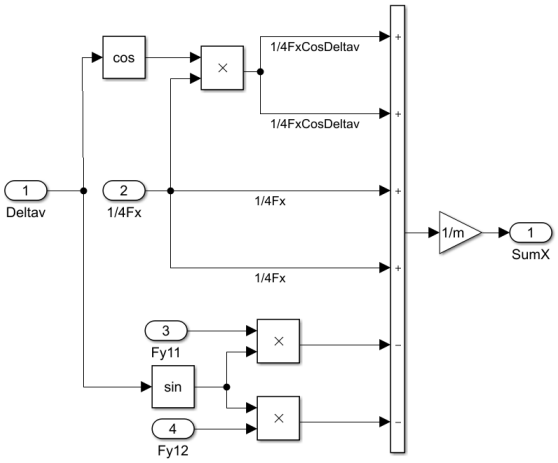

Figure 18.8: Sum of the lateral forces over m

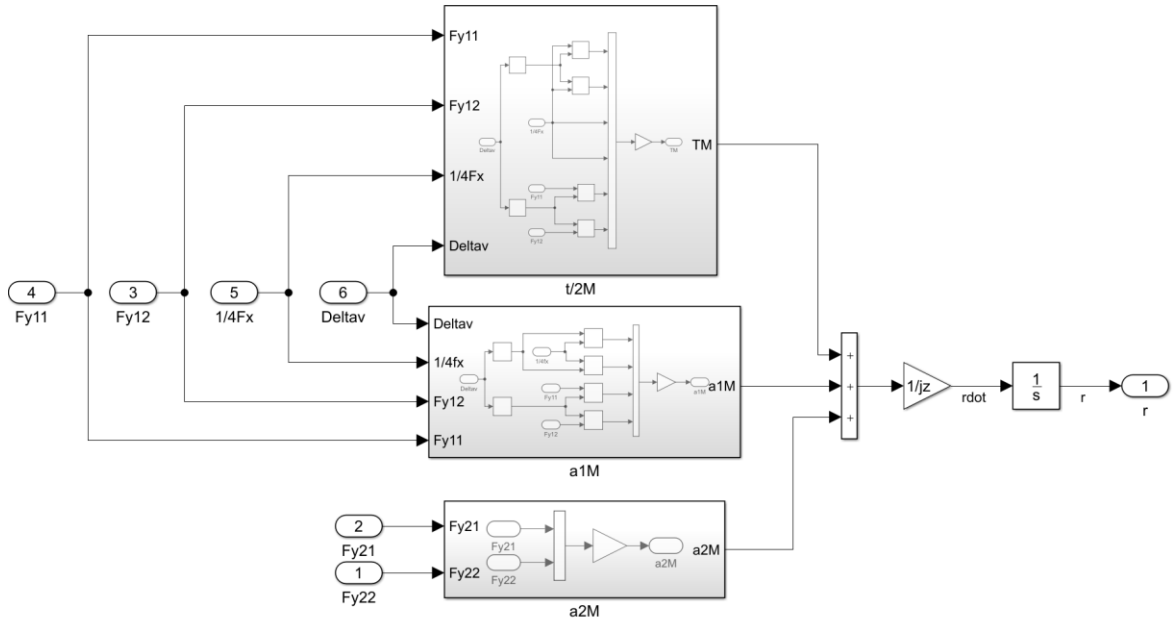

Figure 18.9: Moments

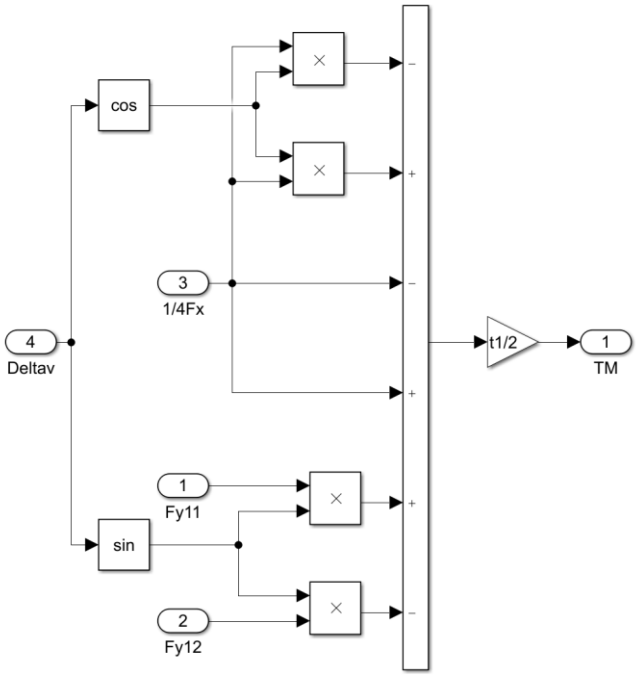

Figure 18.10: Moments multiplied by t/2

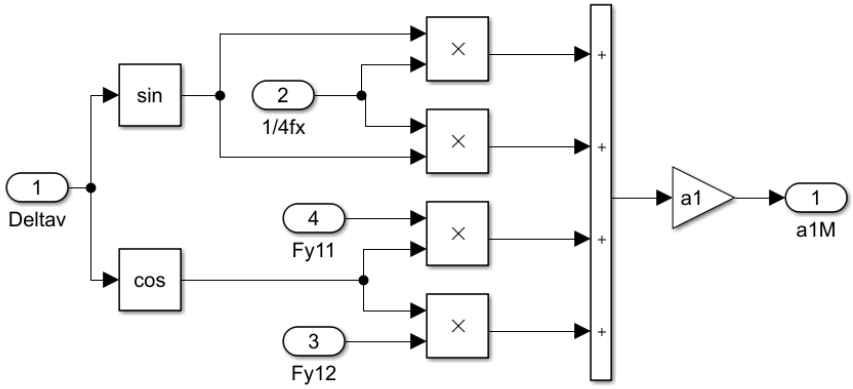

Figure 18.11: Moments multiplied by a1

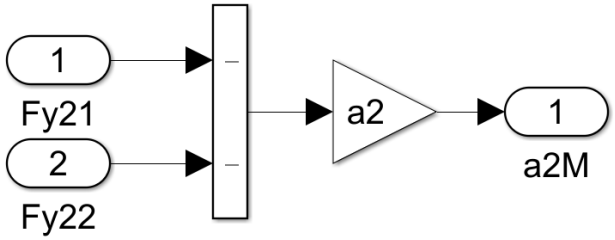

Figure 18.12: Moments multiplied by a2

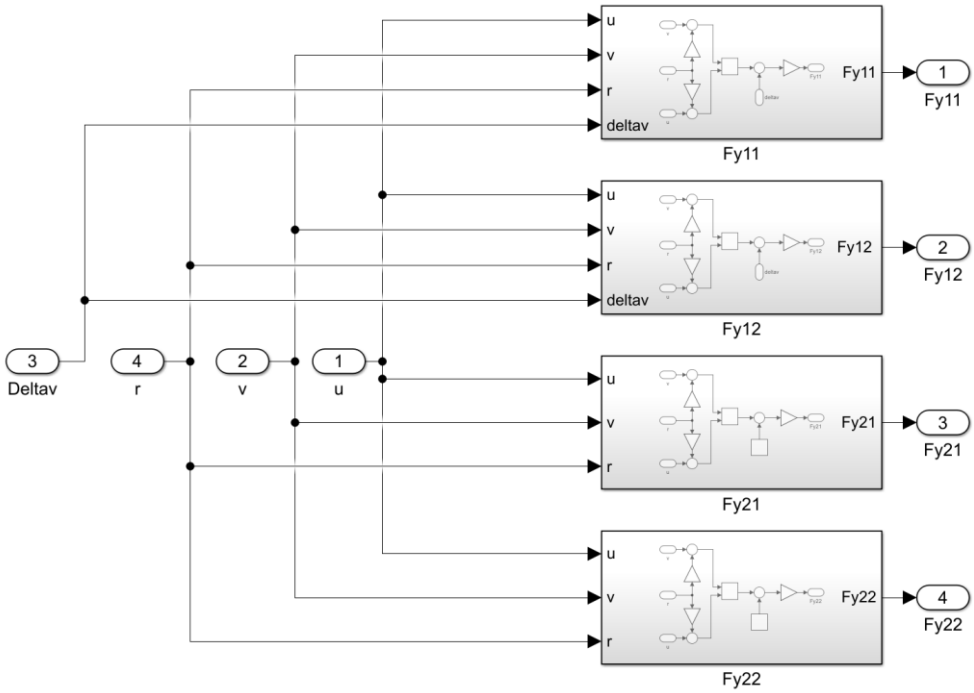

Figure 18.13: Tyre Forces

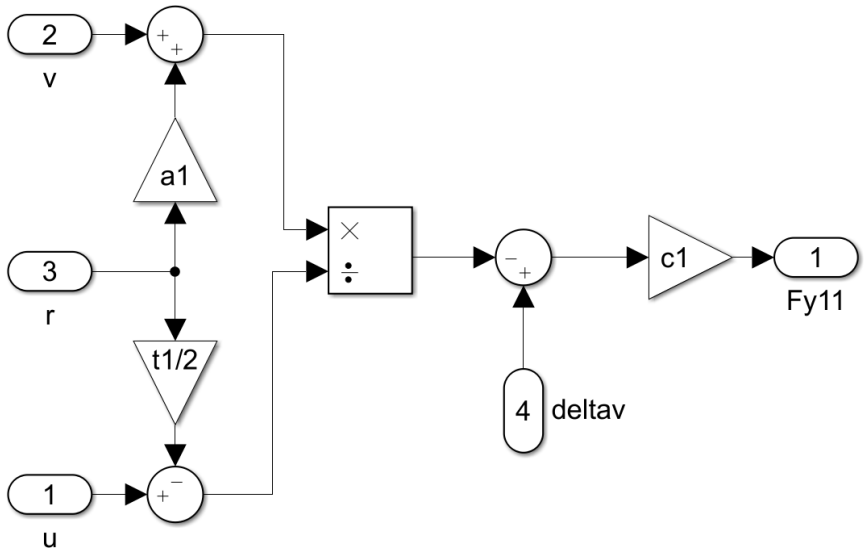

Figure 18.14: Fy11

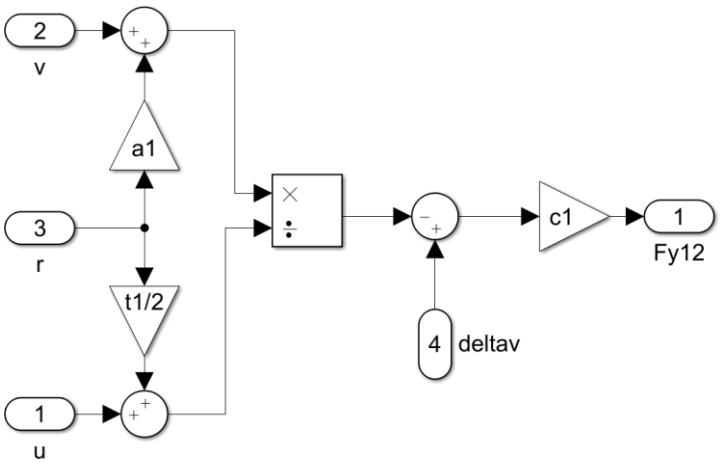

Figure 3.15: Fy12

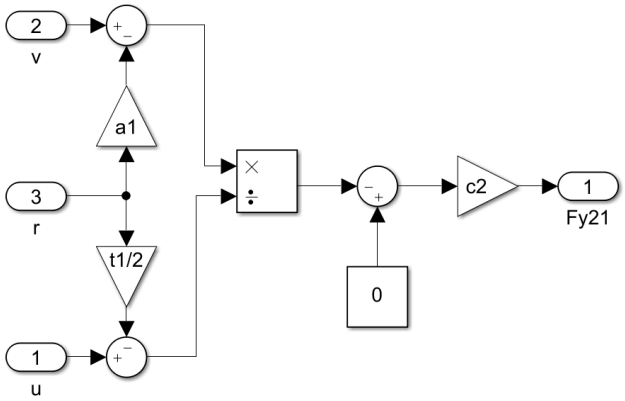

Figure 18.16: Fy21

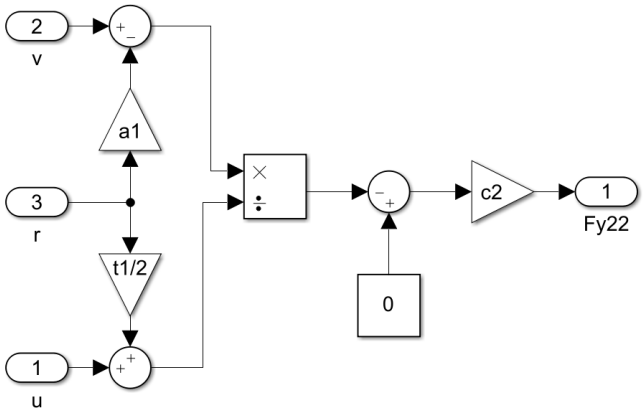

Figure 18.17: Fy22

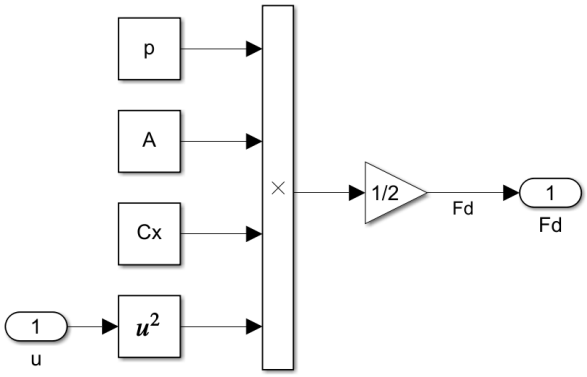

Figure 18.18: Force Drag

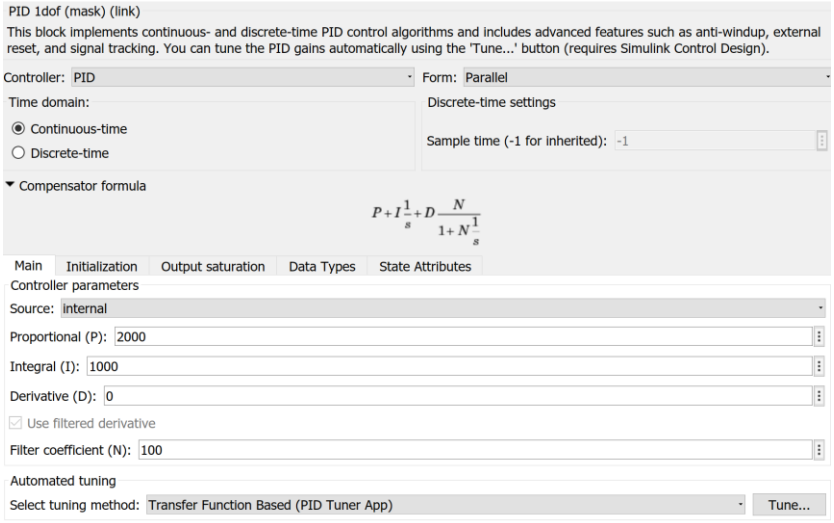

Figure 18.19: PID Parameters

18.3 Preliminary Controller

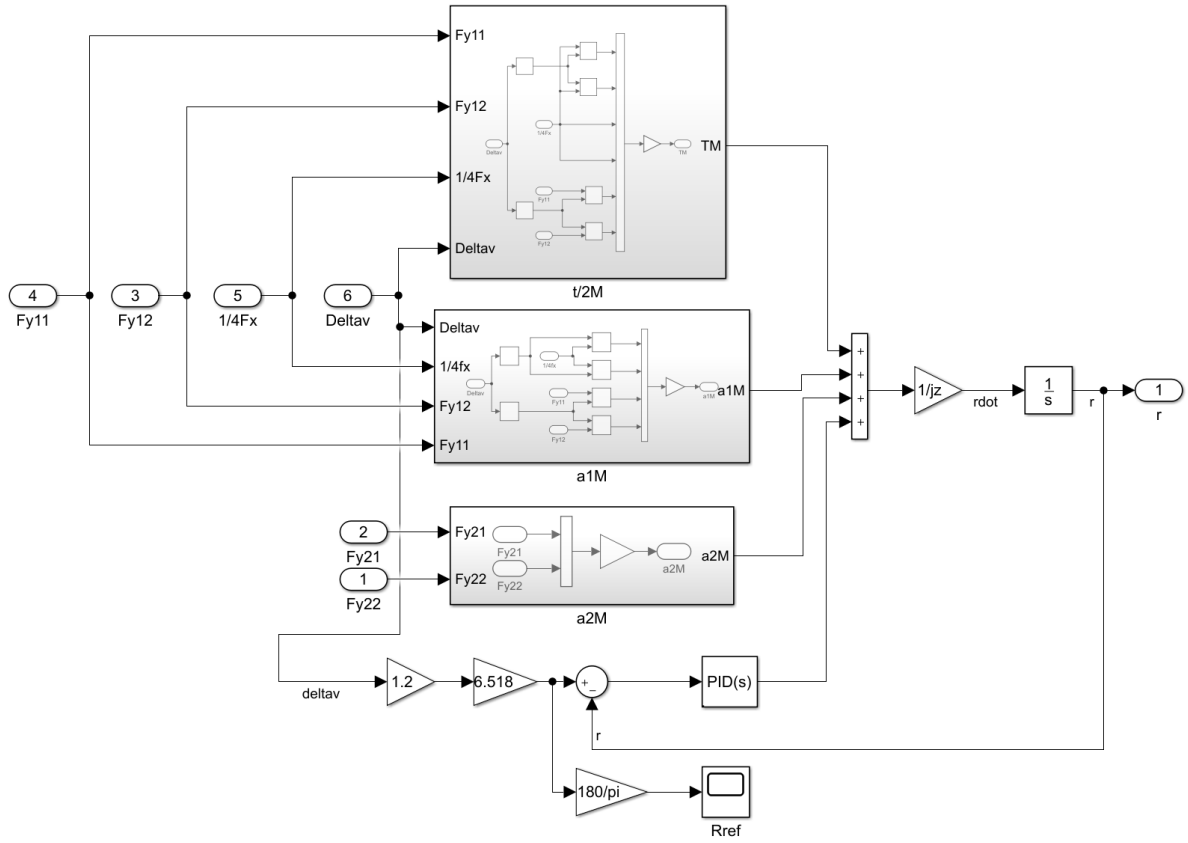

Figure 18.20: Preliminary Controller added to the moments

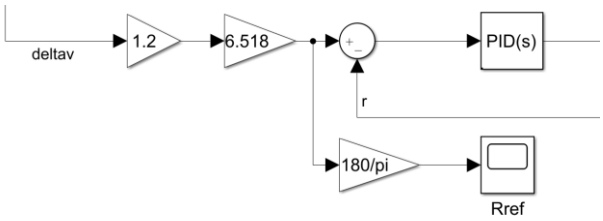

Figure 18.21: Preliminary Controller

18.4 Yaw Rate Controller

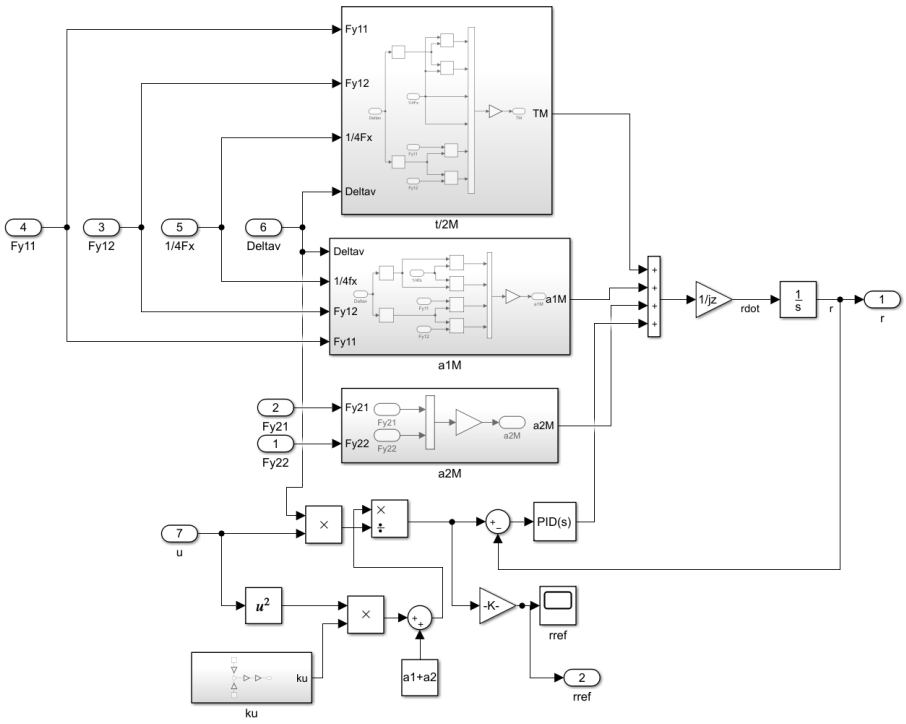

Figure 18.22: Yaw Rate controller added to the moments

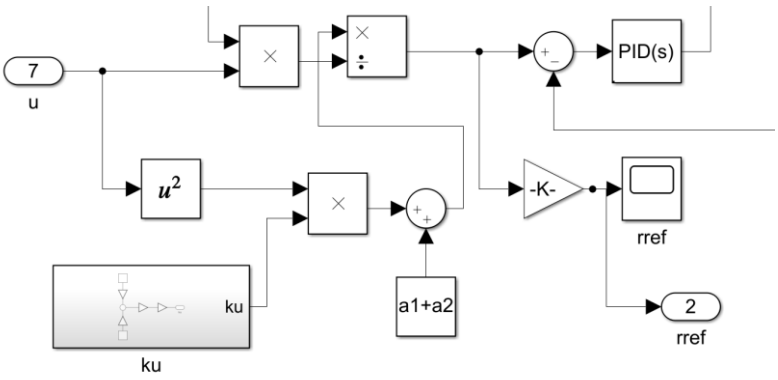

Figure 18.23: Yaw rate controller using the understeering gradient

18.5 Input Signals

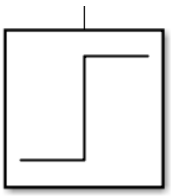

Figure 18.24: Step Response

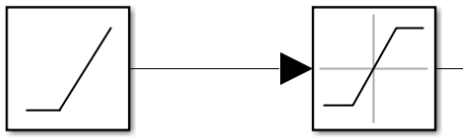

Figure 18.25: Ramp Response

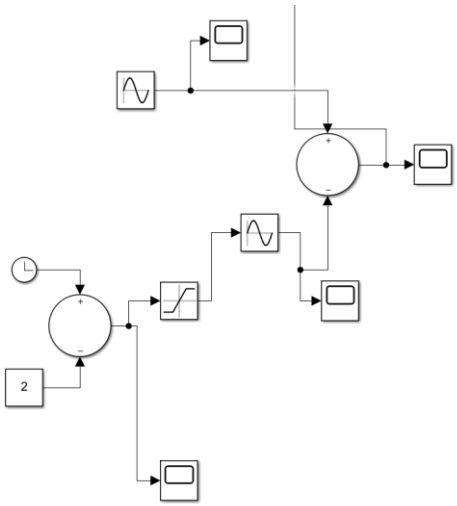

Figure 18.26: Single Lane Change Input

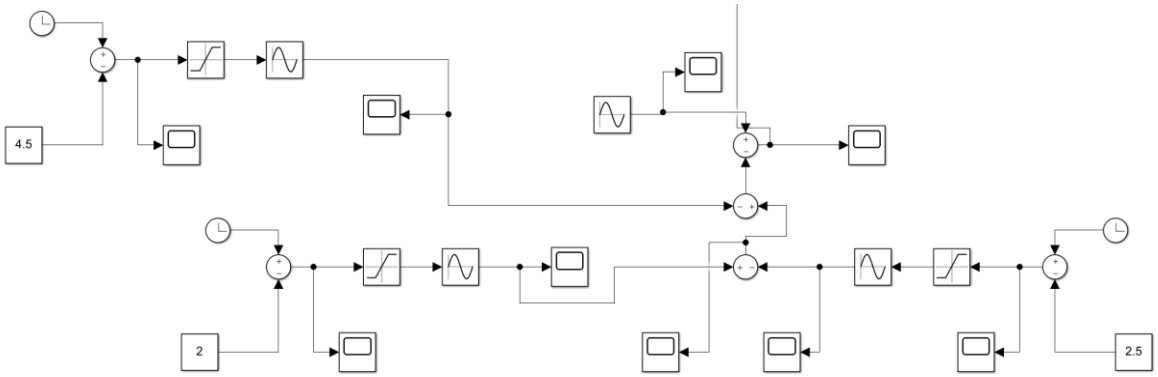

Figure 18.27: Double Lane Change Input

18.5 Gantt Chart